Volume 13
Number 30
14 August 2025
Pages 8943–9298

Journal of Materials Chemistry B

Materials for biology and medicine

rsc.li/materials-b

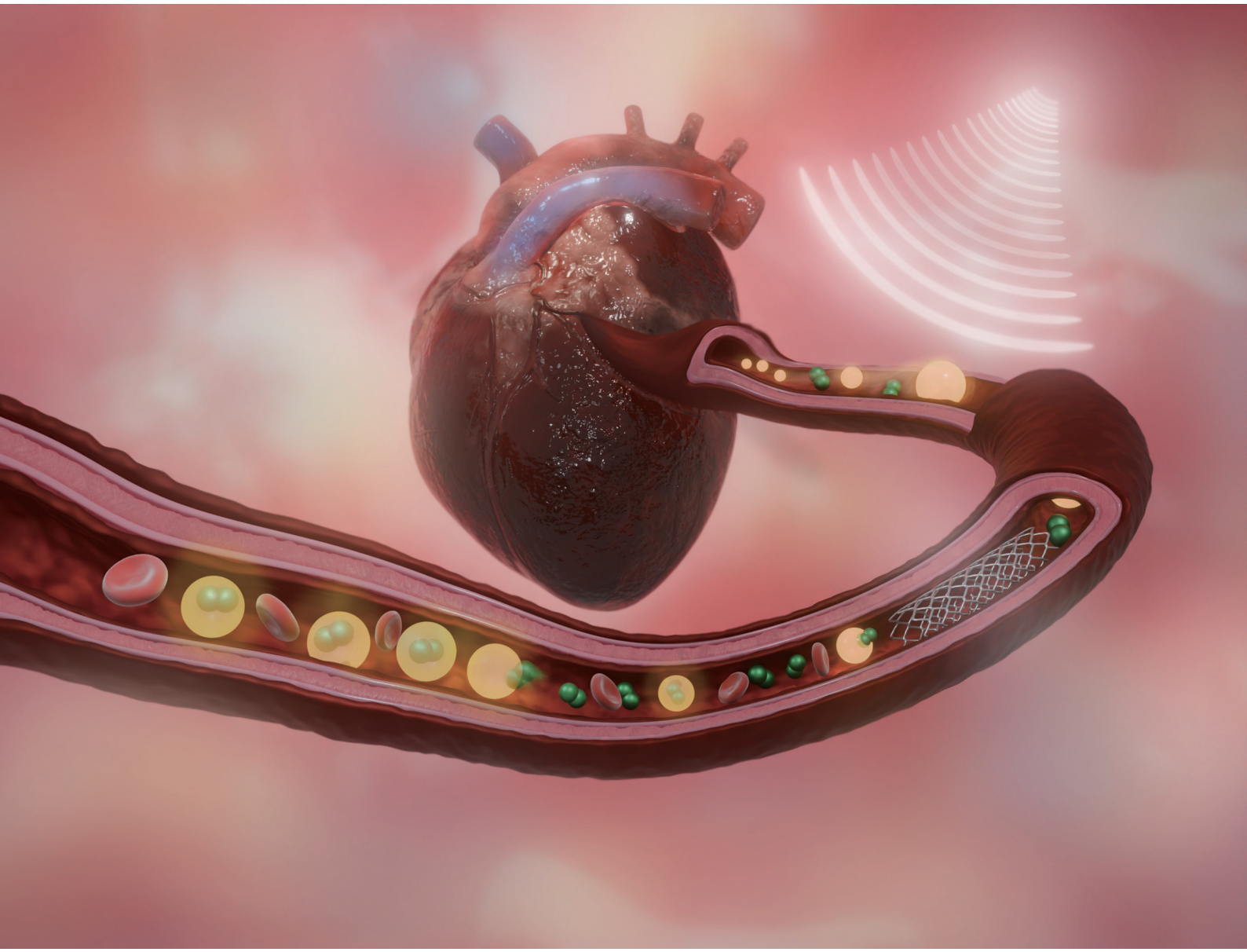

ISSN 2050-750X

ROYAL SOCIETY OF CHEMISTRY

PAPER

Kevin J. Haworth *et al.*

Assessing the oxygen scavenging capacity and myocardial gas embolization risk of ultrasonically activated phase shift perfluorobutane droplets

Journal of Materials Chemistry B

ROYAL SOCIETY OF CHEMISTRY

PAPER

View Article Online
View Journal | View Issue

Cite this: J. Mater. Chem. B, 2025, 13, 9065

Assessing the oxygen scavenging capacity and myocardial gas embolization risk of ultrasonically activated phase shift perfluorobutane droplets†

Nour Al Rifai,[a] Kateryna Stone,[a] Bin Bo,[a] Bin Zhang,[bc] Diviyashree Kasiviswanathan,[c] Andrew N. Redington[bc] and Kevin J. Haworth *[abcde]

This study investigated oxygen scavenging efficiency and the risk of embolization of the cardiac vasculature using ultrasound-triggered phase-shift perfluorobutane (PFB) droplets *in vitro* and *ex vivo*. The emulsion comprised lipid-shelled perfluorobutane core droplets with a modal diameter of 0.98 ± 0.03 μm. The droplets were prepared using a high-pressure microfluidizer. The embolization risk was assessed using a modified *ex vivo* rat Langendorff preparation to accommodate an EkoSonic™ Endovascular Device. The EkoSonic™ Device was composed of an infusion catheter and an ultrasonic core to generate ultrasound at 2.35 MHz and nucleate acoustic droplet vaporization of the droplets. The oxygen scavenging efficiency was studied in an isolated beating heart and an *in vitro* flow phantom setup with target concentrations ranging from 0.05×10^{-4} to 5.0×10^{-4} mL mL^{-1}. Gas embolization from the acoustic droplet vaporization (ADV)-nucleated microbubbles was assessed based on cardiac perfusion and cardiac functional parameters. No change in cardiac perfusion was observed when using droplets with target concentrations below 1.5×10^{-4} mL mL^{-1}, either with or without ultrasound insonation of the droplets. Oxygen scavenging increased with increasing droplet target concentration. The ADV transition efficiency increased with increasing droplet concentration between 0.05×10^{-4} and 0.5×10^{-4} mL mL^{-1} and decreased for higher concentrations. The conclusion of this study was that ultrasound-triggered phase-shift perfluorobutane droplets effectively scavenge oxygen without causing significant embolization at concentrations below 1.5×10^{-4} mL mL^{-1}. Oxygen scavenging increased with higher droplet concentrations, whereas the transition efficiency of ADV reached the largest value at 0.5×10^{-4} mL mL^{-1}, indicating an optimal performance balancing safety and efficacy exists.

Received 5th December 2024,
Accepted 29th April 2025

DOI: 10.1039/d4tb02700k

rsc.li/materials-b

Introduction

Myocardial reperfusion injury is a well-established consequence of treating acute myocardial infarction and other ischemic heart conditions.[1,2] Reoxygenation-dependent injury was discovered in the 1970s[3] leading to the so-called oxygen paradox.[4] Within seconds to minutes after reperfusion, molecular oxygen is converted to excess reactive oxygen species (ROS),[5,6] which are key contributors to reperfusion injury. The reperfusion injury occurs rapidly, such that administering ROS-neutralizing agents at the time of reperfusion is insufficient to prevent reperfusion injury.[4] However, reduced molecular oxygen bioavailability during acute reperfusion can reduce the reperfusion injury based on *ex vivo* studies.[7,8]

Our lab has proposed a new approach to reduce the bioavailability of oxygen in the myocardium during acute reperfusion by modifying dissolved gas content in fluids using acoustic droplet vaporization (ADV). ADV is the phase transition of perfluorocarbon (PFC) liquid droplets to gas microbubbles.[9–13] The resulting microbubbles are potent gas scavengers.[14–16] This strategy holds potential as a targeted and efficient intervention to alleviate the detrimental effects of acute reoxygenation in cardiovascular ischemic diseases, providing new hope in the quest for effective cardioprotective therapies. We envision applying this strategy in the clinical setting using a catheter-based device[17] that could simultaneously establish reperfusion, such as

[a] Department of Internal Medicine, University of Cincinnati, Cincinnati, OH 45267-0586, USA. E-mail: hawortkn@ucmail.uc.edu
[b] Cincinnati Children's Hospital Medical Center, Cincinnati, OH 45229, USA
[c] Department of Pediatrics, University of Cincinnati, Cincinnati, OH 45229, USA
[d] Medical Sciences Baccalaureate Program, University of Cincinnati, Cincinnati, OH 45267-0586, USA
[e] Department of Biomedical Engineering, University of Cincinnati, Cincinnati, OH 45267-0586, USA

† Electronic supplementary information (ESI) available. See DOI: https://doi.org/10.1039/d4tb02700k

via balloon angioplasty, and deliver PFC droplets with ultrasound activation to the same vascular bed.[17]

Kripfgans *et al.*,[12] Kang *et al.*,[18] and Sheeran *et al.*[19] reported that following ADV, gases that had been dissolved in the surrounding fluid can diffuse into the ADV microbubbles. Ingassing occurs due to an approximately 125-fold volumetric expansion of PFC.[12] When PFC droplets are administered outside of the target tissue bed, oxygen can be taken up by the PFC and subsequently delivered to other tissues. Johnson *et al.*[20] demonstrated that liquid perfluoropentane (PFP) droplets alone (*i.e.*, no ADV) can scavenge dissolved oxygen from the surrounding fluid. Culp *et al.*[21] subsequently demonstrated that perfluoropentane (PFP) droplets can transport sufficient oxygen to ischemic tissue to decrease infarct volume in a rabbit stroke model. This effect is not dissimilar to PFC-based blood substitutes, such as Fluosol.[22–24] We have proposed performing ADV in or just proximal to the target tissue *e.g.*, in the left anterior descending coronary artery for treatment of an ST-elevated myocardial infarction.

ADV ingassing is substantial enough to cause as large as a 70 to 80% P_{O_2} reduction in the fluid containing the PFC droplets that undergo ADV.[14,15,25] Increasing the amount of phase transitioned PFC increases oxygen scavenging. Recently, Benton *et al.*[15] demonstrated that ADV of perfluoropentane droplets could be nucleated with a clinically used intravascular ultrasound device, with substantial P_{O_2} reduction.

ADV of PFC droplets has been studied for several other biomedical applications,[12,26–39] including contrast enhanced ultrasound (US) imaging and drug delivery, due to, in part, their stability and hour-long circulation times.[40–42] PFC microbubbles created *via* ADV have been shown to occlude capillary beds and arterioles, which can facilitate embolotherapy in cancer treatment.[12,38,39] The potential of gas embolization increases with increasing microbubble size relative to the vasculature.[43] Interestingly, as oxygen scavenging occurs, the microbubble grows in size.[19,39] Samuel *et al.*[43] and Harmon *et al.*[44] have demonstrated the feasibility and efficacy of using ADV to noninvasively generate emboli within vasculature. ADV embolotherapy involves the accumulation of microbubbles, which are at least 5–6 times larger in diameter than the originating droplets, within the vasculature.[44,45] However, the ability to consistently embolize (occlude) large vessels may be partially dependent on the droplet size and concentration.[46] Although ADV-nucleated gas emboli may be helpful for therapies that benefit from reduced perfusion, it may be detrimental in other therapeutic applications. The use of ADV microbubbles for oxygen scavenging to inhibit reperfusion injury[14,15,25] after restoration of blood supply to the heart is an application where gas embolization could be detrimental. Increasing the droplet concentration would increase the magnitude of oxygen scavenging[15] but may also increase the risk of gas embolization.[44]

Because the oxygen scavenging magnitude depends on the amount of phase transitioned perfluorocarbon, increasing the droplet concentration is necessary for efficient therapy. PFP is commonly used in ADV experiments, but the fraction of PFP droplets undergoing ADV decreases as the droplet diameter decreases. Low-boiling-point PFCs, such as perfluorobutane (PFB, −2 °C), facilitate the use of lower acoustic amplitudes for ADV nucleation than higher boiling point PFCs like PFP (29 °C).[47] Stone *et al.*[16] recently demonstrated that PFB has higher transition efficiency than PFP under the same conditions, supporting the potential of PFB in oxygen scavenging applications.

The aim of this study was to investigate the possibility of using PFB droplets formulated using a lipid shell to achieve oxygen scavenging without causing detrimental cardiac gas embolism. In the first section of this article, PFB droplets were prepared, and size distribution measurements were performed to assess droplet stability and concentration under different storage conditions. In the second section, the risk of gas embolization, assessed by changes in the perfusion flow rate, with these droplets at five different concentrations was studied in a Langendorff preparation using isolated perfused rat hearts with or without ADV. The risk of cardiac dysfunction due to embolization was assessed in the Langendorff preparation *via* metrics of left ventricular pressure. Langendorff-perfused isolated rat heart systems are well-established and highly controlled *ex vivo* models used for the analysis of cardiac function in response to organ injuries or treatments.[48] In the third section, oxygen scavenging using PFB droplets was studied in *ex vivo* isolated hearts and *in vitro* using a flow phantom setup. The *in vitro* oxygen scavenging data were used to calculate the transition efficiency of the five different droplet concentrations studied *ex vivo*.

Materials and methods

Droplet formulation

A droplet emulsion was created with a lipid shell and a core of perfluorobutane. All lipids were purchased from Avanti Polar Lipids (Alabaster, AL, USA) and PFB was purchased from FluoroMed (Round Rock, TX, USA). The outer layer was composed of 1,2-distearoyl-*sn-glycero*-3-phosphocholine (DSPC) and 1,2-distearoyl-*sn-glycero*-3-phosphoethanolamine-*N*-[methoxy-(polyethyleneglycol)-2000] (DSPE-PEG2000), which had been dissolved in chloroform. DSPC and DSPE-PEG2000 were mixed in a molar ratio of 9 : 1 with a total lipid concentration of 3.5 mg mL^{-1} in a glass round bottom flask. Then a thin lipid film was formed on the side of the vial by gently evaporating the chloroform under nitrogen using a rotary evaporator for 1–2 hours. The flask was rotated with the bottom portion placed in a 43 °C water bath. The film was then hydrated with an aqueous excipient solution consisting of phosphate buffered saline (PBS, 1×), propylene glycol, and glycerol at a v/v/v ratio of 16 : 3 : 1. After adding the excipient solution, the flask was submerged in a water bath at 70 °C for 15 min, followed by 30 min of sonication in a bath sonicator (Branson Ultrasonics™ by Thermo Fisher Scientific, Rockford, IL) at 68 °C. The resulting sample was cooled to 4 °C for at least 10 min and no longer than overnight. The lipid solution was subsequently aliquoted with a volume of 2 mL into a 2 mL serum vial and sealed with a butyl septum.

PFB was condensed by flowing PFB gas under a pressure of 20 psi into a 2 mL serum vial cooled on dry ice. Using a

standard 1 mL syringe with a 22-gauge needle, 400 μL of the liquid PFB was drawn up and added to the aliquoted lipid solution through the rubber stopper. The serum vial was kept on ice at 4 °C for 10 min.

A PFB coarse emulsion was formed *via* 45 s of amalgamation using a VIALMIX (Lantheus Medical Imaging, North Billerica, Massachusetts, USA). Following amalgamation, the sample was stored at 4 °C for 20 min to stabilize. The resulting coarse emulsion was pipetted into a 3 mL syringe and processed through direct high-pressure homogenization in an LV1 microfluidizer (Microfluidics International Corporation, Westwood, MA, USA) with both the coil and tray remaining cooled to −15 °C using ice and dry ice baths. The coarse emulsion was passed through the microfluidizer at 13 000 psi once, resulting in PFB droplets. PFB droplets were added in 4 mL aliquots to 6 mL serum vials and sealed.

Droplet sizing

All PFB droplet size distributions were measured in triplicate for three different droplet samples (9 total measurements) using a Multisizer 4 Coulter counter (Beckman Coulter Inc., Brea, CA, USA). Stock solutions of PFB droplets were diluted 1 : 40 000 in filtered (0.2 μm) PBS. A 20 μm aperture tube was used to measure the volume-weighted size distribution between 0.4 and 12 μm, using 200 linearly spaced bins. Volume-weighting was used because it scales with the magnitude of oxygen scavenging.[14–16,25] The volume-weighted modal diameter, concentration (mL of droplets per mL of buffer), and the polydispersity index (PDI, the number-weighted droplet size distribution standard deviation divided by the mean volume-weighted droplet diameter, quantity squared)[16] values were reported. The measured volume-weighted concentration obtained using Multisizer 4 software was scaled by the dilution factors and integrated over all diameters to yield the total droplet volume. The volume of the lipid shell was assumed to be negligible and thus the total PFB volume was estimated to be the same as the total droplet volume.

Sample stability

After preparation, the samples of PFB droplets were stored at 4 °C. These droplet samples were characterized in triplicate using the Multisizer 4, as already described, at the time of manufacture and then approximately every 3 days over 23 days. Three additional samples were stored at room temperature (22.6 ± 0.1 °C). These samples were characterized in triplicate at the time of manufacture and then 5 min, 20 min, 40 min, 60 min, 1 h, 2 h, 3 h, 4 h, and 5 h later.

Nucleation of acoustic droplet vaporization

An EkoSonic™ endovascular device (6 cm treatment zone, 106 cm working length, model 500-55106, Boston Scientific, Inc., Natick, MA, USA) was commercially purchased and used to insonify the infused droplets in order to nucleate ADV. The EkoSonic™ endovascular device consisted of an ultrasonic core with 6 pairs of ultrasound transducer elements.[15] The ultrasonic core was inserted as per the manufacturer's instructions into the provided infusion catheter, designed for disposable clinical use.[49,50] However, for cost-efficiency, the catheters in this study were reused across multiple experiments. The infusion catheter and ultrasonic core were thoroughly flushed using deionized, sterilized water between each trial. As a quality control metric, the electrical impedance of the ultrasonic core was measured daily (Aim4170D, Array Solutions, Sunnyvale, TX, USA), and only ultrasonic cores with a phase between −15° and 10° at 2.35 MHz (the ultrasound insonation frequency) were utilized.[15]

The ultrasonic core of the EkoSonic™ catheter was driven by a 40-cycle tone burst with a burst period of 1.000 ms, using an AFG3500B waveform function generator (Keysight Technologies, Inc., Santa Rosa, CA, USA). A power amplifier was used to obtain a pulse-average electrical drive power of 46.7–47.0 W, corresponding to an estimated peak rarefactional pressure at the exterior surface of the catheter over each transducer pair of 1.5 MPa,[50] the maximum drive power in the FDA-cleared device clinical protocol used for the EkoSonic™ endovascular device.[51] The electrical drive power was computed from the measured impedance of the catheter and voltage applied to the catheter, as measured using an oscilloscope with a 100× reduction probe. The acoustic field pattern emitted by a transducer pair was reported by Lafond *et al.*[49]

Ex vivo Langendorff preparation

All animal procedures were approved by the University of Cincinnati Institutional Care and Use of Animals Committee (protocol 21-10-24-01). Fifty Male Sprague-Dawley rats weighing between 270.6 ± 2.6 grams received Fatal-Plus® (65 mg sodium pentobarbital per mL of solution) administered *via* intraperitoneal injection at a dose of 50 mg kg^{-1} (Patterson Logistics Services, Blythewood, SC, USA). Heparin was used at the same time *via* intraperitoneal injection. After confirming no nociceptor response *via* toe pinch, hearts were rapidly excised using a standard technique[52] and mounted onto a Langendorff perfusion apparatus (Fig. 1). The hearts were perfused under recirculating conditions, maintaining a perfusion pressure of 78 ± 4 mmHg. The perfusate was Krebs–Henseleit buffer (KHB); composed of 119 NaCl, 4.7 KCl, 1.2 $MgSO_4$, 1.25 $CaCl_2$, 1.2 KH_2PO_4, 25 $NaHCO_3$, and 11 glucose (all values in millimolar [mM]). Prior to use, the buffer was subjected to vacuum filtration using a 1 μm filter to remove any particulate matter. This solution was continuously bubbled with a mixture of 95% O_2 and 5% CO_2 to maintain a stable pH of 7.4 and a consistent oxygen partial pressure of 523 ± 34 mmHg. The temperature of the oxygenated KHB was rigorously maintained within the range of 36.5 to 37.5 °C going into the heart using water jacketing. The dissolved oxygen (P_{O_2}) and temperature were measured with a flow-through sensor (TOFTC2, PyroScience GmbH, Aachen, Germany) integrated into the system just proximal to the heart. Left ventricular pressure was recorded using a standard left ventricular balloon and pressure sensor.[52] Cardiac function, including left ventricular developed pressure (LVDP), the rate of contraction and release (maximal and minimal dp/dt), and left ventricular end diastolic pressure (LVEDP), were computed using LabChart. Perfusion flow rate was recorded (Transonic Systems Inc., Ithaca, NY, USA).

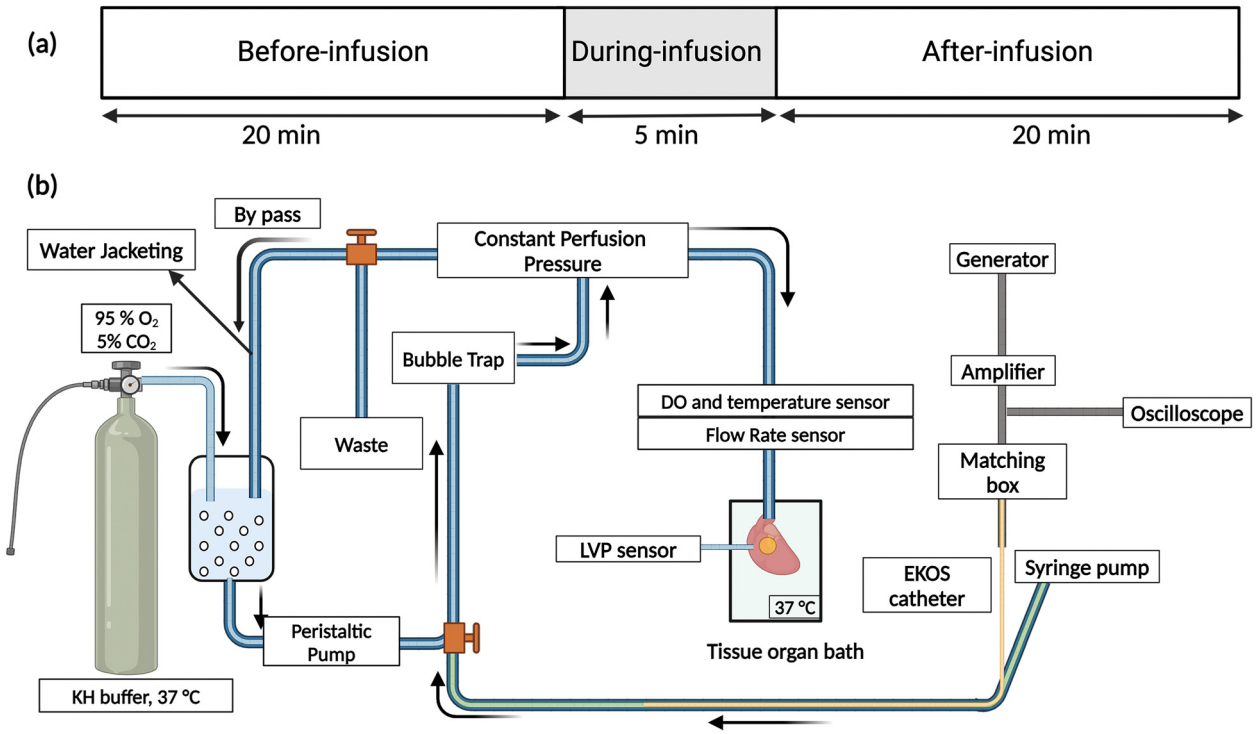

Fig. 1 (a) Timeline of Langendorff perfusion for isolated rat hearts. (b) Schematic diagram of the Langendorff apparatus. The Langendorff apparatus featured a reservoir of oxygenated KHB (partial pressure of oxygen (P_{O_2}) of 523 ± 34 mmHg). KHB was pumped through the system in tubing (cyan) within water-jacketing (blue) to ensure a temperature of 37 °C. Cardiac function assessment utilized a balloon placed in the left ventricle, while perfusion flow rate was monitored through an in-line flow probe. Droplets were introduced into the Langendorff system *via* a syringe pump through the coolant lumen of the EkoSonic™ infusion catheter. The water jacketing tubing was filled with KHB. The EkoSonic™ ultrasonic core (yellow) was also inserted through the coolant lumen. A 2.35 MHz pulsed ultrasound tone burst was applied to the droplets using a 6 cm treatment zone EkoSonic™ ultrasound core. The P_{O_2} in the buffer entering the heart was measured using a flow-through oxygen sensor. (Created with **https://BioRender.com**.)

Cardiac function and flow rate were recorded using PowerLab and LabChart (ADInstruments, North America, Colorado Springs, CO, USA) throughout the experiment.

The standard constant pressure Langendorff preparation was modified to enable infusion of the PFB droplets through an EkoSonic™ endovascular device following an initial 20 min stabilization phase (Fig. 1a). Droplets were infused through the coolant port of the EkoSonic™ infusion catheter at 5 mL min^{-1}. The EkoSonic™ infusion catheter was placed in a tubing filled with KHB using a hemostasis valve and surrounded by water jacketing to maintain a temperature of 37 °C. The tubing with the EkoSonic™ infusion catheter joined the Langendorff setup distal to the peristaltic pump but proximal to the bubble trap (designed to trap macrobubbles[52] and not microbubbles) (Fig. 1b). The flow rate from the peristaltic pump was 16 mL min^{-1}, so the droplets were diluted by a factor of 3.2 when mixed. The bubble trap was placed above the heart to achieve a constant perfusion pressure head. A bypass at the bubble trap allowed the perfusion flow rate to be determined by the resistance of the heart. This setup enabled a consistent droplet dilution independent of fluctuations in perfusion flow rate. The droplet stock concentration was measured and appropriately diluted in KHB to achieve target concentrations of droplets entering the heart for each experiment. The volume-weighted droplet target concentrations perfusing the heart were 0.25×10^{-4}, 0.5×10^{-4}, 1.5×10^{-4}, 2.5×10^{-4}, and 5×10^{-4} mL mL^{-1}. These target concentrations were selected based on prior studies of ADV-mediated oxygen scavenging performed by Benton *et al.*[15] Droplet infusions lasted for 2 min. The EkoSonic™ infusion catheter was primed with KHB. The time taken for the solution to travel from the EkoSonic™ infusion catheter's tip to the flow-through sensor was approximately 1 min. Subsequently, a 20-minute period of recovery and stabilization ensued (Fig. 1a). Dissolved oxygen, perfusion flow rate, and cardiac function measurements were acquired in real-time throughout each experiment. If the perfusion flow rate and cardiac function measurements dropped by greater than 90% for several minutes, the heart was assumed to be in an unrecoverable injury and the experiment ended early.[52]

The data for each experiment could be grouped into three distinct phases: before infusion (syringe pump for droplet infusion off), during infusion (syringe pump for droplet infusion on and the time taken for the droplets to flow from the catheter to the heart) and after infusion (syringe pump and EkoSonic™ ultrasound core off and no droplets are anticipated to still be flowing in the system) (Fig. 1a). The during infusion period occurred either without ultrasound to determine the effect of droplets or with ultrasound to determine the effect of microbubbles formed *via* ADV. All experiments involving P_{O_2} measurements were repeated six times unless otherwise noted.

In vitro flow phantom setup

An *in vitro* flow phantom, previously used to investigate ADV-based oxygen scavenging with droplets[15] (Fig. 2), was used to measure ADV-mediated oxygen scavenging and calculate the ADV transition efficiency of droplets. Briefly, a peristaltic pump was used to circulate oxygenated deionized water through the flow phantom at a flow rate of 16 mL min^{-1}. The oxygenated de-ionized water was prepared in a covered 4 L reservoir by constantly bubbling a 95%/5% O_2/CO_2 gas mixture. The oxygenated water's temperature was maintained in the range of 36.5 to 38.0 °C with a water bath and water jacketing. The corresponding P_{O_2} of the oxygenated deionized water was 553 ± 8 mmHg. An EkoSonic™ endovascular device was used to both infuse droplets and nucleate ADV using the same ultrasound parameters reported in the *ex vivo* Langendorff section. The effect of droplet concentration on the oxygen scavenging was measured using the same in-line oxygen sensors. The target volume-weighted droplet concentrations were 0.0×10^{-4} (no droplet, negative control), 0.05×10^{-4}, 0.25×10^{-4}, 0.5×10^{-4}, 2.5×10^{-4} and 5×10^{-4} mL mL^{-1}. *In vitro* experiments were performed with the droplets infused through the catheter for 1 min before ultrasound insonation so that the effect of the droplets on oxygen scavenging could be determined separately from the effect of ADV. Ultrasound remained turned on until a steady state of P_{O_2} was achieved. This approach was not feasible in the *ex vivo* hearts due to the potential cumulative effect on the heart of droplets and microbubbles formed *via* ADV (*e.g.*, droplet or gas embolization).

Transition efficiency calculation

A physics-based model was used to estimate the droplet transition efficiency. The model of Radhakrishnan *et al.*[14,15] was inverted to estimate the volume of perfluorobutane transitioned from liquid to gas based on the measured oxygen partial pressures before ADV and during ADV and the measured droplet concentration in the sample reservoir without ultrasound exposure.[14] The ratio of other gasses, such that the sum of the partial pressures in the model was 760 mmHg, was based on humidified air. Thus, there were 154.6 mmHg, 0.3 mmHg, 59.4 mmHg, 7.1 mmHg, and 47 mmHg of O_2, CO_2, N_2, Ar, and H_2O, respectively. A temperature of 37 °C was assumed in the model. The solubility of oxygen was assumed to be 964 L atm per mol in water.[53,54] The effect of PFB solubility in buffer (1.5 mg L^{-1} (ref. 55)) was neglected when calculating transition efficiencies because, at the lowest concentration, only approximately 4% of the liquid PFB would dissolve into the buffer. The volumetric expansion factor (162.12×) was calculated based on the change in density of liquid and gaseous perfluorobutane (liquid PFB density: 1517 kg m^{-3} and gas density: 9.93 kg m^{-3}).[56,57] Surface tension and viscosity were not considered for the numerical model.

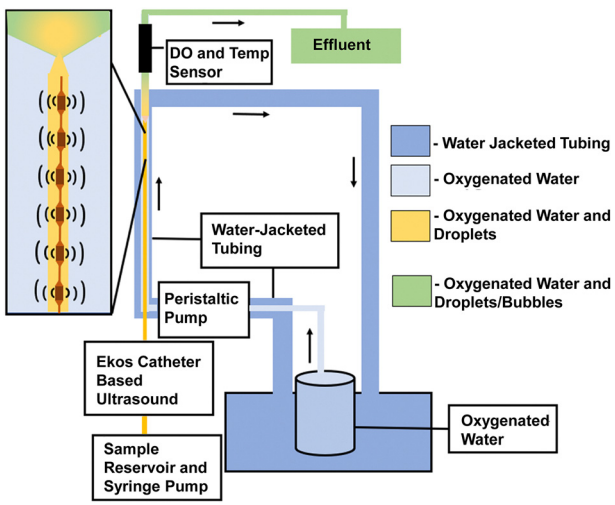

Fig. 2 Schematic diagram of the *in vitro* flow phantom. The oxygenated deionized water reservoir and tubing were warmed. Droplets were infused through the flow system using a syringe pump through an EkoSonic™ infusion catheter, which was maintained at 37 °C. The oxygenated water had an initial partial pressure of oxygen (P_{O_2}) of 553 ± 8 mmHg. A 2.35 MHz pulsed ultrasound tone burst (40 cycles) insonified the droplets using a 6 cm treatment zone EkoSonic™ ultrasonic core. The P_{O_2} in the fluid downstream of the catheter was measured using a flow-through oxygen sensor. The figure was reproduced from Benton *et al.*,[15] which used an identical setup.

Data analysis

All presented data are expressed as the mean ± standard error mean (SEM). Thermal stability at 22 °C and storage stability at 4 °C were assessed through mixed-effect models. *P*-values less than 0.05 were considered statistically significant.

Cardiac function was assessed *via* coronary perfusion flow, left ventricular developed pressure (LVDP), left ventricular end diastolic pressure (LVEDP), and the maximum rate of contraction (maximal d*p*/d*t*) and relaxation (minimal d*p*/d*t*). The LVDP, flow rate, maximal d*p*/d*t*, minimal d*p*/d*t* and LVEDP were averaged every 1 min for the whole 45 min of experiments. Cardiac function parameters were derived from measured left ventricular pressure using built-in functions within LabChart. Cardiac function and oxygen scavenging relative to baseline values (*i.e.*, before infusion) were analysed at two-time windows. The first window was designed to capture the transient effects of droplet infusion (either with or without ultrasound). Within the five minutes immediately following the start of droplet infusion (*i.e.*, the during infusion period), the timepoint of maximum change relative to the average stabilization (*i.e.*, the before infusion period) was determined and the cardiac function at this point was compared to the average value of the final five minutes of the before infusion period. The fraction of hearts with less than 10% change (*i.e.*, minimal effect) was tallied. The second window compared the average value of the last five minutes of the before infusion period and the average value of the last five minutes of the after-infusion period. The second window was used to assess cardiac function recovery. This timepoint was analysed in two ways: (1) a non-inferiority test with a margin of 10% and (2) calculation of the fraction of hearts with less than 10% decrease between before infusion and after infusion values. A change in perfusion of 90% for 15 minutes or greater results in cardiomyocyte death.[58] The threshold of 10% was selected based on a pilot study assessment of variability observed in cardiac function during the before droplets infusion time period and to serve as a very

conservative safety margin. These analyses were performed for each experimental group. For oxygen scavenging, a 5% margin for the non-inferiority test was used to assess the change in oxygen partial pressure before infusion and after infusion based upon the variability observed during the before droplets infusion time period in pilot experiments. In all cases, the null hypothesis was that the difference between before infusion and after infusion was greater than the margin. A mixed effect model was used to compare *in vitro* oxygen scavenging amounts with and without ultrasound considering the correlation of multiple measurements within the same subject. Comparison of the transition efficiencies for different droplet concentrations was assessed using a one-way ANOVA test with a Tukey correction for multiple comparisons.

Results

Droplet size distribution and concentration

The PFB coarse emulsion had a volume-weighted concentration and a polydispersity index of $1.9 \times 10^{-2} \pm 6.4 \times 10^{-4}$ mL mL^{-1} and 0.91 ± 0.04, respectively (Fig. 3a). Note that the 20 μm Multisizer 4 aperture used for these measurements was unable to capture the complete size distribution of the coarse emulsion, which included droplets greater than 12 μm or smaller than 0.4 μm and therefore may underestimate the concentration and polydispersity index. After high-shear homogenization, the droplet emulsion was less polydisperse than the coarse emulsion, with a modal diameter of 0.98 ± 0.03 μm (Fig. 3b). The droplet emulsion solution volume-weighted concentration and the polydispersity index (PDI) were $3.7 \times 10^{-2} \pm 0.5 \times 10^{-2}$ mL mL^{-1} and 0.13 ± 0.02, respectively.

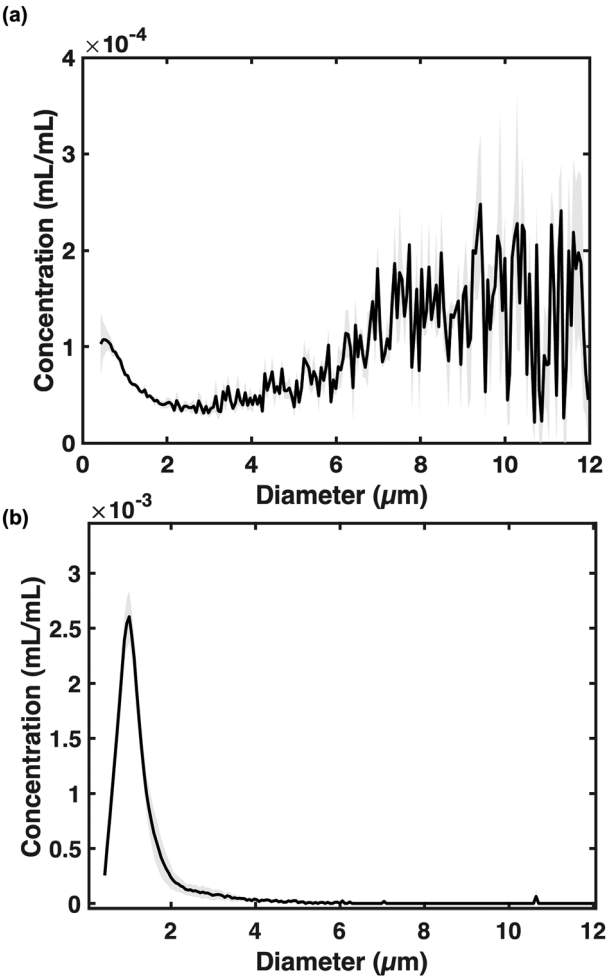

Fig. 3 Volume-weighted distribution of (a) the coarse emulsion droplet solution and (b) droplets emulsion solution after one passage of high shear pressure homogenization at 10 000 PSI. The droplet emulsion had a nominal modal diameter of 0.98 ± 0.03 μm. The lines and shading are the mean and standard error mean, respectively (N = 4 for both measurements).

Droplet storage stability at 4 °C

To evaluate droplet stability under storage conditions, undiluted samples were placed in a laboratory refrigerator (4 °C). Droplets settled to form a pellet, however, no visible phase separation was observed when the emulsion was swirled to resuspended and measured. No statistically significant changes in concentration, modal diameter, or polydispersity index were observed for the PFB droplets stored in the fridge over time (4 °C) (Fig. 4). All subsequent storage of droplets following manufacturing was at 4 °C.

Droplet room temperature stability

To determine if the PFB droplet concentration or diameter changed during preparation on the day of a flow phantom experiment, the samples were diluted 40 000× in PBS and placed on a lab bench (22.6 °C ± 0.1 °C). The droplet concentration and size distribution remained stable for 5 h (Fig. 5). All subsequent experiments were performed within 5 h of removal from storage. No statistically significant changes in concentration, modal diameter, or polydispersity index were observed over 5 hours.

Cardiac function with and without droplets and ultrasound

Following the start of droplet infusion, any changes in cardiac function were delayed by 1–2 minutes due to the temporal duration it takes the flow to go from the end of the EkoSonic™ infusion catheter to the heart (grey shaded region, Fig. 1a). Table 1 illustrates the number of hearts with and without ultrasound exposure that had changes in cardiac function or oxygenation of the perfusion buffer of less than 10% or 5%, respectively, relative to the average value over the last 5 minutes of the before infusion period. When comparing the before infusion and during infusion periods, the minimum of the during infusion period was used. When comparing the before-infusion and after-infusion periods, the average of the last five minutes of the after-infusion period was used. The data indicate that decreased droplet concentration is correlated with an increased fraction of hearts exhibiting less than 10% changes in cardiac function.

The change in average perfusion flow rate relative to the last 5 min of stabilization is shown without (Fig. 6a) and with ultrasound exposure (Fig. 6b). Tables 2 and 3 provide the average flow rate during the final 5 minutes before infusion,

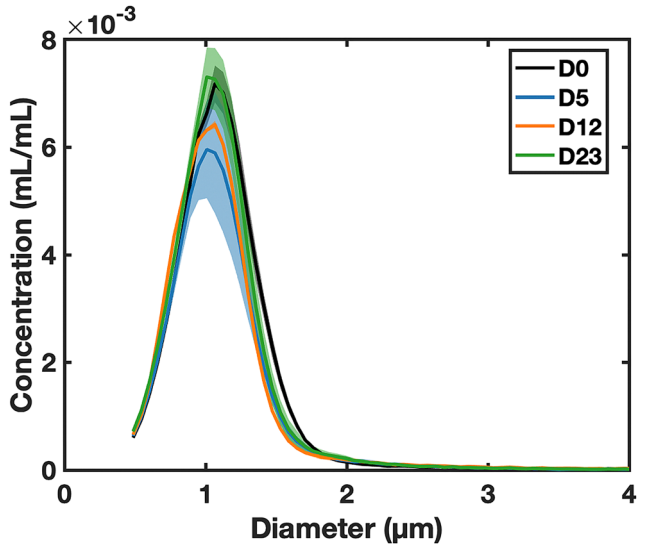

Fig. 4 Size distribution of droplet emulsion solutions stored at 4 °C during 23-day storage. The days post manufacturing are indicated in the legends where D0 is the day of droplet manufacturing. Each line is the average of n = 3 measurements. The lines and shading are the mean and standard error mean of the triplicate measurements, respectively.

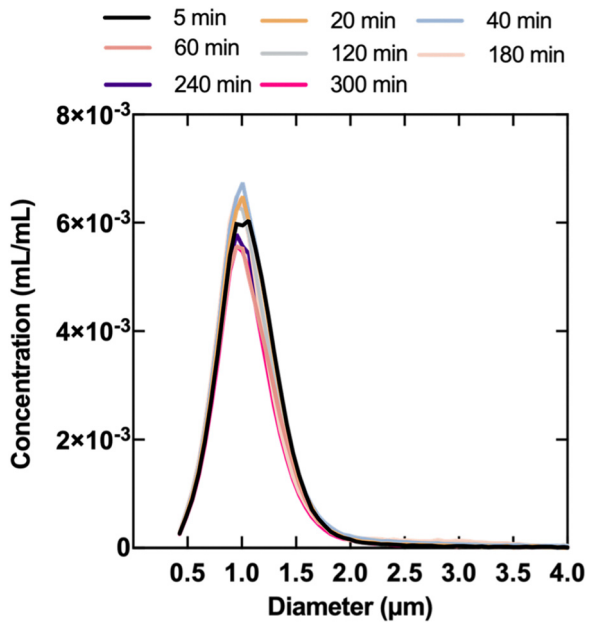

Fig. 5 PFB droplet concentration as a function of time at room temperature (22.6 °C ± 0.1 °C) up to 5 h. Each line is the average of n = 3 measurements.

the minimum value during the 5 min following the start of infusion, and the final 5 minutes after infusion for each concentration with and without ultrasound. At 5.0 × 10^{-4} mL mL^{-1} without ultrasound, one heart of four had a flow rate that dropped from 17 mL min^{-1} to 10 mL min^{-1} between 40 and 45 min, resulting in the large standard deviations observed in Fig. 6a. For all concentrations without and with ultrasound the

Table 1 Number of hearts for which cardiac function (perfusion flow rate and LVDP) and oxygen partial pressure changed by less than 10% or 5%, respectively, relative to stabilization during infusion and after infusion at 5 different droplet concentrations (0.25 × 10^{-4}, 0.5 × 10^{-4}, 1.5 × 10^{-4}, 2.5 × 10^{-4}, and 5 × 10^{-4} mL mL^{-1}) with and without ultrasound exposure. The total number of hearts for each droplet concentration is shown in the left column. A different heart was used for each trial

	Without ultrasound		With ultrasound	
Droplet concentration (mL mL^{-1}, ×10^{-4})	During infusion Δ < 10%	After infusion Δ < 10%	During infusion Δ < 10%	After infusion Δ < 10%
Perfusion flow rate				
0.25 (N = 6)	5	5	0	4
0.5 (N = 6)	6	5	0	4
1.5 (N = 6)	2	4	0	3
2.5 (N = 5)	0	1	0	0
5.0 (N = 4)	2	0	—	—
LVDP				
0.25 (N = 6)	1	6	0	4
0.5 (N = 6)	4	4	1	5
1.5 (N = 6)	2	4	0	5
2.5 (N = 5)	0	2	0	0
5.0 (N = 4)	0	0	—	—
Oxygen partial pressure				
0.25 (N = 6)	2	6	0	6
0.5 (N = 6)	0	6	0	5
1.5 (N = 6)	0	6	0	6
2.5 (N = 5)	0	4	0	0
5.0 (N = 4)	0	0	—	—

p-value of the non-inferiority test was greater than 0.05, indicating that the flow rate significantly decreased by more than 10% when comparing after infusion to before infusion.

The change in average LVDP relative to the last 5 min of stabilization is shown without (Fig. 7a) and with ultrasound exposure (Fig. 7b). The average LVDP during the final 5 minutes before infusion, the minimum value during the 5 min following the start of infusion, and the final 5 minutes after infusion for each concentration with and without ultrasound are listed in Tables 2 and 3. For all concentrations without and with ultrasound the p-value of the non-inferiority test was greater than 0.05 except for 0.25 × 10^{-4} mL mL^{-1}, indicating that the LVDP significantly decreased more than by 10% when comparing after infusion to before infusion.

The cardiac function left ventricular contraction rate (maximal dp/dt), left ventricular relaxation rate (minimal dp/dt) and left ventricular end diastolic pressure (LVEDP) during each experiment were determined with and without ultrasound and are reported in the ESI† (Fig. S1–S3 and Tables S1, S2). For droplet infusion without ultrasound, the minimum values of cardiac parameters (LVEDP, maximal dp/dt, and minimal dp/dt) during the 5 minutes following infusion were compared to the average values from the final 5 minutes before infusion. At the lowest concentrations (0.25 × 10^{-4} mL mL^{-1}, 0.5 × 10^{-4} mL mL^{-1}, and 1.5 × 10^{-4} mL mL^{-1}), no changes were observed, showing that droplet infusion had minimal effect. However, at higher concentrations (2.5 × 10^{-4} mL mL^{-1} and 5 × 10^{-4} mL mL^{-1}), a noticeable effect was seen. When comparing the average values from the 5 minutes post-infusion

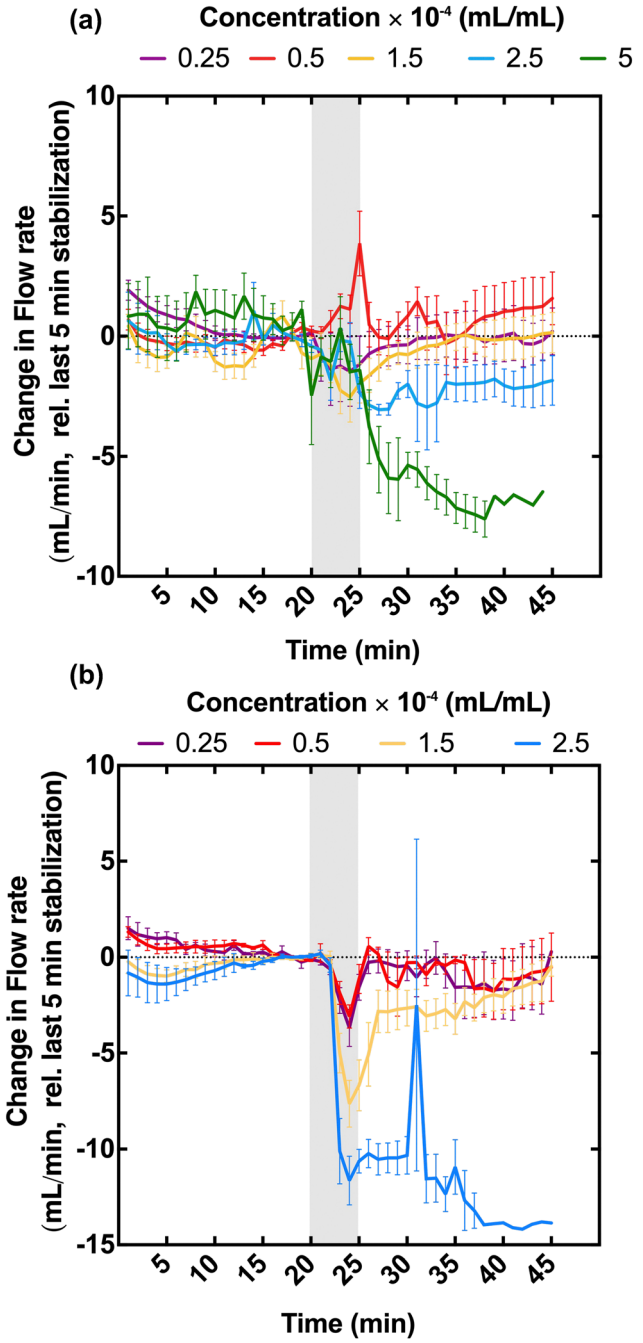

Fig. 6 The change in the perfusion flow rate relative to the last 5 min of stabilization throughout the 45 min experiments without (a) and with (b) ultrasound exposure for five different droplet concentrations (0.25×10^{-4}, 0.5×10^{-4}, 1.5×10^{-4}, 2.5×10^{-4}, and 5×10^{-4} mL mL^{-1}). The first 20 min of the experiment was the stabilization phase (before infusion). The grey shaded area on the graph demarks the 2 min of droplet infusion (during infusion) followed by a 3 min period that accounts for approximately 1 min to infuse the dead volume of the EkoSonic™ infusion catheter and the time to flow from the end of the catheter to heart. The time from 25 min to 45 min represents the heart recovery period (after infusion). Each value is mean ± SEM, 6 hearts per group, except for 2.5×10^{-4} mL mL^{-1} where 5 hearts were used and 5×10^{-4} mL mL^{-1} where only 4 hearts were used without ultrasound due to three of four hearts ceasing perfusion before the 45 min time point. Using reduced animal numbers was deemed ethical.

Table 2 Average perfusion flow rate, LVDP, and oxygen partial pressure during the final 5 minutes before infusion, the minimum value during the 5 min following the start of infusion, and the final 5 minutes after infusion at 5 different droplet concentrations (0.25×10^{-4}, 0.5×10^{-4}, 1.5×10^{-4}, 2.5×10^{-4}, and 5×10^{-4} mL mL^{-1}) without ultrasound

Droplet concentration (mL mL^{-1}, $\times 10^{-4}$)	Without ultrasound		
	Final 5 minutes before infusion	Minimum value during infusion	Final 5 minutes after infusion
Flow rate (mL min^{-1})			
0.25	10 ± 1	8 ± 1	9 ± 1
0.5	11 ± 0	11 ± 0	13 ± 1
1.5	10 ± 1	7 ± 0	10 ± 2
2.5	9 ± 0	6 ± 0	7 ± 1
5	11 ± 2	9 ± 1	3 ± 2
LVDP (mmHg)			
0.25	90 ± 10	74 ± 8	92 ± 10
0.5	101 ± 4	93 ± 2	95 ± 10
1.5	95 ± 3	71 ± 7	91 ± 9
2.5	92 ± 6	54 ± 11	70 ± 11
5	94 ± 7	40 ± 8	8 ± 2
Oxygen partial pressure (mmHg)			
0.25	535 ± 9	468 ± 9	552 ± 6
0.5	486 ± 15	411 ± 22	497 ± 24
1.5	518 ± 4	477 ± 16	556 ± 4
2.5	542 ± 4	433 ± 4	516 ± 10
5	445 ± 2	280 ± 15	310 ± 66

Table 3 Average perfusion flow rate, LVDP, and oxygen partial pressure during the final 5 minutes before infusion, the minimum value during the 5 min following the start of infusion, and the final 5 minutes after infusion at 5 different droplet concentrations (0.25×10^{-4}, 0.5×10^{-4}, 1.5×10^{-4}, 2.5×10^{-4}, and 5×10^{-4} mL mL^{-1}) with ultrasound

Droplet concentration (mL mL^{-1}, $\times 10^{-4}$)	With ultrasound		
	Final 5 minutes before infusion	Minimum value during infusion	Final 5 minutes after infusion
Flow rate (mL min^{-1})			
0.25	9 ± 1	6 ± 0	9 ± 2
0.5	8 ± 1	5 ± 0	8 ± 1
1.5	10 ± 1	2 ± 1	9 ± 1
2.5	12 ± 1	0 ± 0	1 ± 1
LVDP (mmHg)			
0.25	96 ± 5	55 ± 5	96 ± 16
0.5	76 ± 7	41 ± 3	80 ± 11
1.5	108 ± 8	35 ± 6	117 ± 16
2.5	100 ± 9	24 ± 3	19 ± 6
Oxygen partial pressure (mmHg)			
0.25	525 ± 8	440 ± 6	544 ± 6
0.5	529 ± 4	435 ± 3	535 ± 15
1.5	533 ± 7	390 ± 5	546 ± 4
2.5	537 ± 4	352 ± 13	353 ± 33

to those from the 5 minutes pre-infusion, concentrations of 0.25×10^{-4} mL mL^{-1}, 0.5×10^{-4} mL mL^{-1}, 1.5×10^{-4} mL mL^{-1}, and 2.5×10^{-4} mL mL^{-1} showed less than 10% change. However, at 5×10^{-4} mL mL^{-1}, cardiac dysfunction was observed, similar to the changes seen in LVDP and perfusion flow rate. This dysfunction was characterized by a

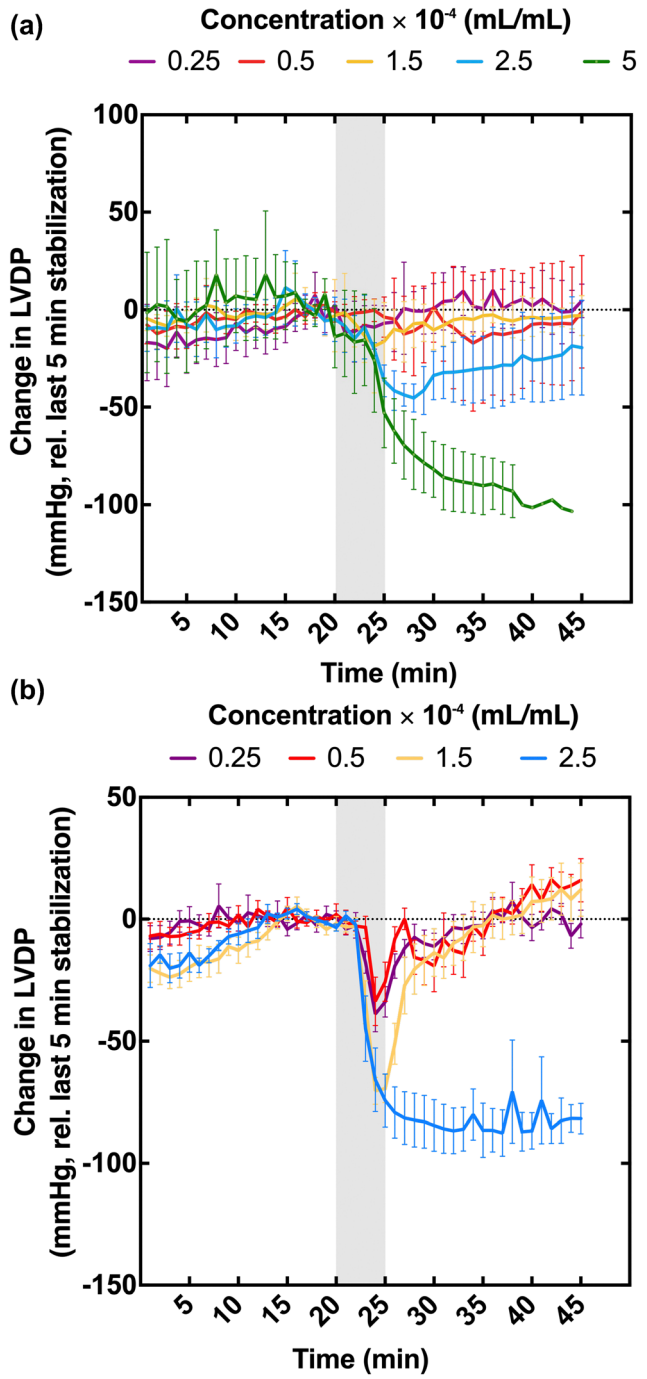

Fig. 7 The change in left ventricular developed pressure (LVDP) relative to last 5 min of stabilization throughout the 45 min experiments without (a) and with (b) ultrasound exposure for five different droplet concentrations (0.25×10^{-4}, 0.5×10^{-4}, 1.5×10^{-4}, 2.5×10^{-4}, 5×10^{-4} mL mL^{-1}). The first 20 min of the experiment was the stabilization phase (before infusion). The grey shaded area on the graph demarks the 2 min of droplet infusion (during infusion) followed by a 3 min period that accounts for approximately 1 min to infuse the dead volume of the EkoSonic™ infusion catheter and the time to flow from the end of the catheter to heart. The time from 25 min to 45 min represents the heart recovery period (after infusion). Each value is mean ± SEM, 6 hearts per group, except for 2.5×10^{-4} mL mL^{-1} where 5 hearts were used and 5×10^{-4} mL mL^{-1} where only 4 hearts were used without ultrasound due to three of four hearts ceasing perfusion before the 45 min time point. Using reduced animal numbers was deemed ethical.

decrease in LVDP, perfusion flow rate, and maximal dp/dt, alongside an increase in LVEDP and minimal dp/dt.

For droplet infusion with ultrasound, the minimum values of cardiac parameters during the 5 minutes following infusion were again compared to the average values from the 5 minutes before infusion. Here, LVEDP, maximal dp/dt, and minimal dp/dt showed a consistent trend similar to that observed in LVDP and perfusion flow rate. Droplet infusion had an observable effect on LVEDP at concentrations of 0.25×10^{-4} mL mL^{-1}, 0.5×10^{-4} mL mL^{-1}, 1.5×10^{-4} mL mL^{-1}, and 2.5×10^{-4} mL mL^{-1}. When comparing the averages of the 5 minutes after infusion to the averages of the 5 minutes before infusion, less than a 10% change was observed for concentrations of 0.25×10^{-4} mL mL^{-1}, 0.5×10^{-4} mL mL^{-1}, and 1.5×10^{-4} mL mL^{-1}. At 2.5×10^{-4} mL mL^{-1}, cardiac dysfunction, similar to that observed in LVDP and perfusion flow rate, was noted. The cardiac dysfunction was characterized by a decrease in LVDP, perfusion flow rate, and maximal dp/dt, and an increase in LVEDP and minimal dp/dt, suggesting the onset of ischemic conditions in heart tissue.

Ex vivo effect of droplet concentration on ADV-mediated oxygen scavenging

The change in average P_{O_2} relative to the last 5 min of stabilization is shown in Fig. 8a and b without and with ultrasound exposure, respectively. The magnitude of the P_{O_2} decreased with increasing droplet volume-weighted concentration (Tables 2 and 3). Table 1 illustrates the number of hearts with and without ultrasound exposure, where the change in oxygenation was less than 5% when comparing the last 5 minutes of the before infusion period to the minimum of the during infusion period or the last five minutes of the after-infusion period.

For droplet concentrations 2.5×10^{-4} mL mL^{-1} and 5×10^{-4} mL mL^{-1} without ultrasound the p-value of the non-inferiority test was greater than 0.05, indicating the P_{O_2} decreased more than 10% when comparing the after-infusion to before-infusion periods. When droplets were infused with the EkoSonic™ ultrasonic core activated at a concentration of 2.5×10^{-4} mL mL^{-1} the p-value of the non-inferiority test was greater than 0.05, indicating that the P_{O_2} value decreased by more than 10% when comparing the after-infusion to before-infusion periods.

In vitro effect of droplet concentration on ADV-mediated oxygen scavenging

The oxygen scavenging magnitude for droplets at the six different target concentrations (0.0×10^{-4} (no droplet, negative control), 0.05×10^{-4}, 0.25×10^{-4}, 0.5×10^{-4}, 2.5×10^{-4}, and 5×10^{-4} mL mL^{-1}) in the *in vitro* flow phantom setup are shown in Fig. 9. With droplets but without ultrasound exposure, there was no significant difference in oxygen scavenging ($p > 0.05$) in P_{O_2} between most target concentrations except for 0.05×10^{-4} and 0.25×10^{-4} mL mL^{-1} ($p = 0.0049$) as well as between and 0.05×10^{-4} and 5.0×10^{-4} mL mL^{-1} ($p = 0.0142$). For each target concentration except for 0.0×10^{-4} (no droplet, negative control) and 0.05×10^{-4}, the amount of oxygen

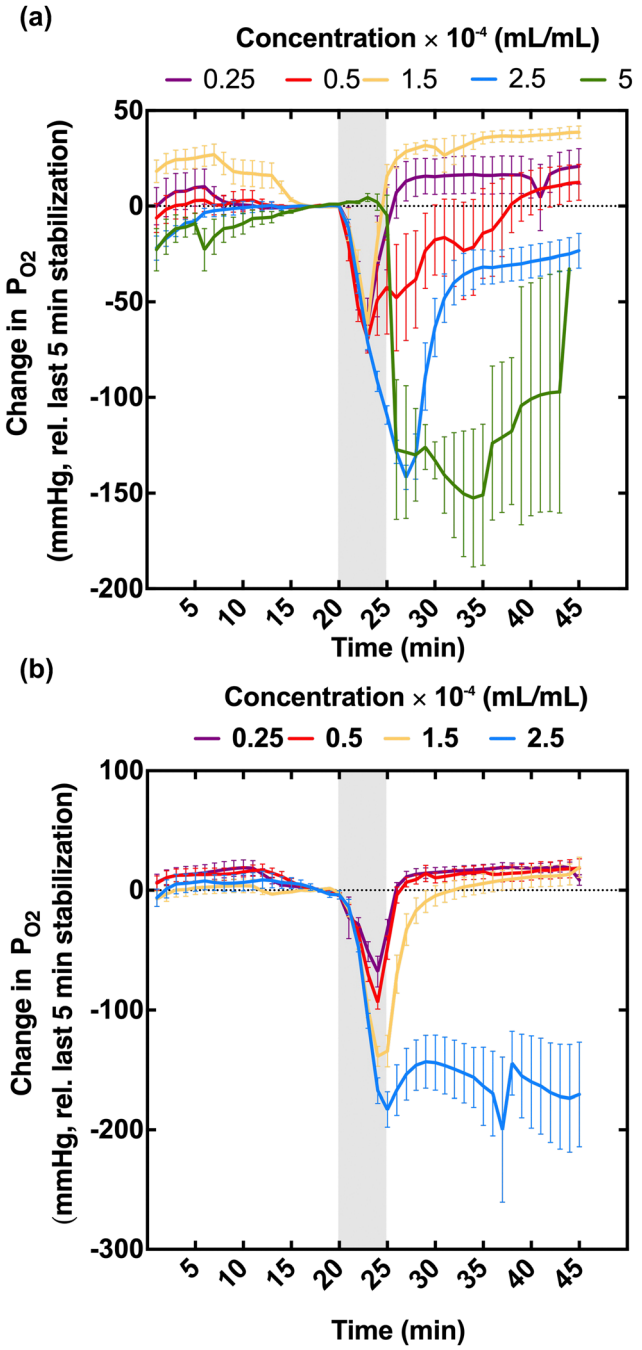

Fig. 8 The change of partial pressure of oxygen (P_{O_2}) relative to the last 5 min of stabilization throughout 45 min of perfusion without ADV (a) and with ADV (b), respectively using the Langendorff apparatus for 5 different droplet concentrations (0.25×10^{-4}, 0.5×10^{-4}, 1.5×10^{-4}, 2.5×10^{-4}, 5×10^{-4} mL mL^{-1}). The first 20 min of the experiment was the stabilization phase (before infusion). The grey shaded area on the graph demarks the 2 min of droplet infusion (during infusion) followed by a 3 min period that accounts for approximately 1 min to infuse the dead volume of the EkoSonic™ infusion catheter and the time to flow from the end of the catheter to heart. The time from 25 min to 45 min represents the heart recovery period (after infusion). Each value is mean ± SEM, 6 hearts per group, except for 2.5×10^{-4} mL mL^{-1} where 5 hearts were used and 5×10^{-4} mL mL^{-1} where only 4 hearts were used without ultrasound due to three of four hearts ceasing perfusion before the 45 min time point. Using reduced animal numbers was deemed ethical.

scavenged with ultrasound compared to without ultrasound exposure had a p-value less than 0.007, indicating a statistically significant difference. This indicates there was more oxygen scavenging from ADV than from spontaneous droplet vaporization. The infusion of water with ultrasound (0.0×10^{-4} mL mL^{-1}, no droplet, negative control), led to a slight 4 mmHg reduction in P_O, which was not statistically significant (p = 0.078). The total oxygen scavenging (with droplets and ultrasound (solid bars)) increased with increasing droplet target volume-weighted concentration. A significant difference (p-value <0.05) between all target concentrations except 2.5×10^{-4} and 5.0×10^{-4} mL mL^{-1}. The total oxygen scavenging increased from 73 ± 21 mmHg at 0.05×10^{-4} mL mL^{-1} to 373 ± 42 mmHg at 2.5×10^{-4} mL mL^{-1}.

Transition efficiency

The calculated ADV transition efficiency for the target concentrations of 0.05×10^{-4}, 0.25×10^{-4}, 0.5×10^{-4}, 2.5×10^{-4}, and 5×10^{-4} mL mL^{-1} was based on the *in vitro* oxygen scavenging measurements from Fig. 9, and was plotted in Fig. 10. The transition efficiency initially increased (5.8 ± 4.8%, 49.6 ± 36.7%, and 78.2 ± 12.6%) with droplet target concentration for 0.05×10^{-4} mL mL^{-1} to 0.25×10^{-4} mL mL^{-1} and 0.5×10^{-4} mL mL^{-1}, respectively. It then decreased to 46.4 ± 18.1% for 2.5×10^{-4} mL mL^{-1} and to 16.3 ± 2.6% for 5×10^{-4} mL mL^{-1}. A significant difference was observed between all target concentrations except for 0.25×10^{-4} mL mL^{-1} *versus* 2.5×10^{-4} mL mL^{-1} and 0.05×10^{-4} *versus* 5×10^{-4} mL mL^{-1}.

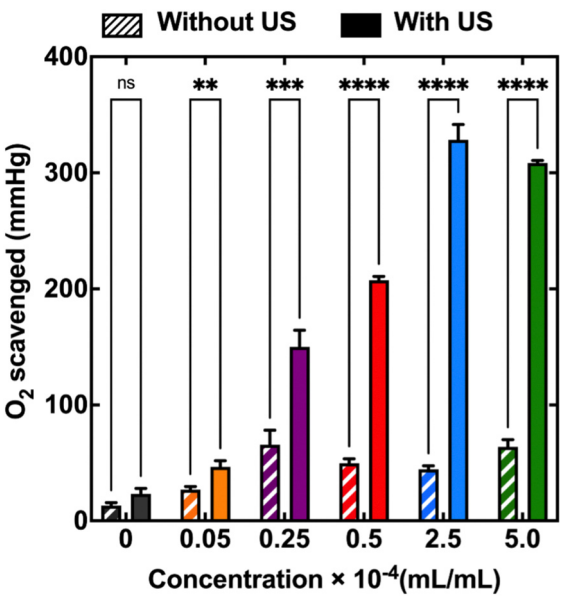

Fig. 9 The magnitude of oxygen scavenging before- and during-ADV using the *in vitro* flow phantom setup with droplet concentrations of 0.0×10^{-4} (no droplet, negative control), 0.05×10^{-4}, 0.25×10^{-4}, 0.5×10^{-4}, 2.5×10^{-4}, and 5×10^{-4} mL mL^{-1}. The hashed bars represent oxygen scavenging observed without ultrasound (before ADV). The solid-colored bars are the amount of oxygen scavenging observed with ultrasound (during ADV).

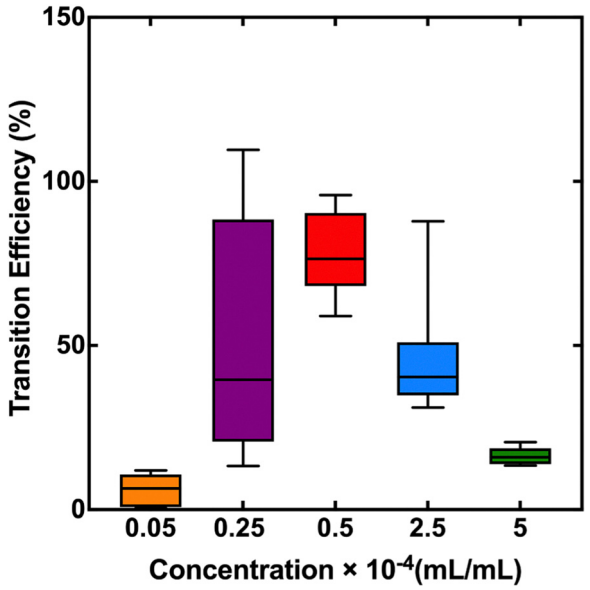

Fig. 10 The calculated ADV transition efficiency for the five different target droplet concentrations 0.05×10^{-4}, 0.25×10^{-4}, 0.5×10^{-4}, 2.5×10^{-4}, 5×10^{-4} mL mL^{-1}. The transition efficiency was calculated based on the change in the partial pressure of oxygen after droplet infusion with and without ADV using the Radhakrishnan model.[14]

Discussion

The research presented here was motivated by the long-term need to create perfluorocarbon droplets that could be used for ultrasound-activated oxygen scavenging *via* intravascular delivery to inhibit cardiac reperfusion/reoxygenation injury. Upon exposure to ultrasound of sufficient pressure amplitude, perfluorocarbon droplets can be converted into echogenic gas-filled microbubbles through a process termed acoustic droplet vaporization (ADV).[12,19,59] In the model of Radhakrishnan *et al.*[14] as the volume fraction of ADV microbubbles in a fluid increases, so too does the magnitude of oxygen scavenged from the surrounding fluid. However, a large amount of gas can cause embolization.[38,39,43,44,60] Therefore, this study was specifically designed to investigate both oxygen scavenging and risk for gas embolization for ~0.9 μm diameter PFB droplets. High-shear homogenization was demonstrated to be useful for the manufacturing of stable PFB droplets. The droplets can be stored for at least 3 weeks with a minimal change in the concentration or diameter. The volume and concentrations of droplets produced were sufficient to enable studies on oxygen scavenging and gas embolization. The PFB droplets statistically scavenged significant amounts of oxygen from the buffer in which they were diluted, potentially due to spontaneous droplet vaporization. The droplets exposed to ultrasound caused either transient or prolonged changes to cardiac function depending on the concentration used.

Droplet manufacturing and size characteristics

Manufacturing PFB droplets using a high shear pressure homogenizer produced a stable, low polydispersity emulsion with a high concentration (Fig. 3b). The methods used are based on the work of de Gracia Lux *et al.* and the results are generally consistent with their findings.[61] However, the methods presented herein used different settings on an LV1 homogenizer, which likely explains the larger droplets observed in this study as compared to the study of de Gracia Lux *et al.*[61] During homogenization, the coarse emulsion suspension is passed through an interaction chamber under high pressure (10 000 psi), and fragmented into droplets by the cavitation turbulence, shear-forces associated with velocity gradients.[62] The PFB core remains condensed after passing it through LV1 at 10 000 psi. This can be attributed to the increased hydrostatic pressure applied during homogenization, which is much greater than the Laplace pressure.[63,64]

The volume fraction of PFB in the total solution prior to forming the coarse emulsion was 16.67×10^{-2} mL mL^{-1} (0.4 mL of PFB per 2.4 mL of the total solution). The final droplet stock solution had a volume fraction of $3.7 \times 10^{-2} \pm 0.5 \times 10^{-2}$ mL mL^{-1}. Thus, approximately 78% of the PFB was unaccounted for. Based on flow cytometry measurements by Stone *et al.*[16] 0.3–0.4% of droplets were smaller than 0.40 μm in diameter and thus would not have been detected based on our use of the Multisizer 4 with a 20 μm aperture. The remainder of the unaccounted PFB was likely lost during manufacturing due to the volatility of PFB.

Droplet stability

Stability is an essential requirement for low-boiling point PFC-in-water droplets to be of practical use and is commonly studied.[25,61,65–68] It is known that temperature may impact the stability of droplets by increasing their volatility as the temperature increases.[64] Both the sizing and concentration data over the course of the 5 h test period revealed the stability of PFB droplets when exposed to room temperature (Fig. 5). PFB droplets were stable for up to 23 days with respect to both size distribution and concentration when stored at 4 °C. This finding aligns with the finding by Yarmoska *et al.*,[69] who demonstrated that proper PEGylation is crucial for stabilizing droplets, reducing the risk of coalescence.

Cardiac function in response to PFC droplet infusion

The function of an isolated heart is often described by factors such as flow rate, LVDP, and the rate of change of pressure during contraction (+dp/dt) and relaxation (minimal, or peak −dp/dt).[52,70] The research presented herein was designed to assess the cardiac risk of gas embolization from nominally 0.98 μm PFB droplets and ADV-nucleated microbubbles. Thus, the primary cardiac parameter of interest is the perfusion flow rate. Varying the perfluorocarbon emulsion's size and concentration was demonstrated to result in occlusion of flow following ADV.[38,39,43] Fig. 6 demonstrates that the change in perfusion flow rate had either no or only a transient change while droplets were flowing through the heart both with and without ultrasound exposure for concentrations of 0.25×10^{-4} mL mL^{-1}, 0.5×10^{-4} mL mL^{-1}, and 1.5×10^{-4} mL mL^{-1}. However, a notable and persistent decline in perfusion flow rate

occurred at concentrations of 2.5×10^{-4} mL mL^{-1} (with ultrasound) and 5×10^{-4} mL mL^{-1} (without ultrasound). The change in LVDP mirrored observations for decreased absolute perfusion flow rate. LVDP is a frequently used metric of overall cardiac performance in Langendorff preparations, but is difficult to interpret as it reflects a composite of changes in the systolic and diastolic performances of the heart. Nevertheless, there was a significant effect of infusing the droplets, at all concentrations, on LVDP. Interestingly, LVEDP was relatively unaffected during the infusion period, suggesting that the primary effect was to reduce the systolic performance of the heart. Changes in dp/dt are a more sensitive measure of cardiac contractility and relaxation. With regard to the latter, both +dp/dt and −dp/dt were similarly significantly reduced at higher droplet concentrations ($>2.5 \times 10^{-4}$ mL mL^{-1}), but were relatively unaffected, even during the infusion period, without ultrasound activation. However, with activation, there was a significant, transient, effect on cardiac function at all concentrations. While the magnitude of the effect was lower at lower concentrations, and full recovery to baseline occurred within approximately 30 minutes at concentrations $\leq 1.5 \times 10^{-4}$ mL mL^{-1}, these transient effects on cardiac function will need to be taken into account if this strategy translates into clinical therapy. For the droplet concentrations resulting in sustained decreases in flow rate, a delayed but important elevation of the LVEDP was observed. This result, in combination with reduced perfusion, indicates that the tissue became ischemic, impairing relaxation, and increasing myocardial stiffness.[71,72] Overall, these results establish clear upper limits for the concentrations of this formulation of approximately 0.98 μm diameter PFB droplets that can be used in cardiac tissue. It should be noted that the lipid shell composition may affect these results. Sabnis *et al.*[73] demonstrated that cholesterol enhances membrane stability and reduces droplet fusion, resulting in uniform particle sizes. Similarly, Tam *et al.*[74] showed that phospholipids such as DSPC and DPPC increase droplet rigidity, which contributes to stability and uniformity. Exploring alternative shell materials or modifying droplet size could enable higher concentrations without triggering gas embolization.

Effect of droplet concentration on ADV-mediated oxygen scavenging

Similar to the work of Benton *et al.*,[15] it was observed that as the droplet concentration increased, the magnitude of oxygen scavenging increased until a saturation point, such that droplets with concentrations of 2.5×10^{-4} mL mL^{-1} and 5.0×10^{-4} mL mL^{-1} scavenged similar amounts of oxygen. Although comparable, Benton *et al.* found that the saturation point occurred at 5.0×10^{-4} mL mL^{-1} and greater concentrations. Notably, Benton *et al.* used larger (3, 5, and 7 μm *versus* 0.9 μm) perfluoropentane (rather than perfluorobutane) droplets. The higher boiling point of PFP and thus a lower anticipated transition efficiency could explain the differences between Benton *et al.* and the present study. Kawabata *et al.* demonstrated that the ADV pressure amplitude threshold depends on the perfluorocarbons used.[11] However, based on the findings of Benton *et al.*, the transition efficiency decreases for smaller droplets, which potentially offsets the benefit of using perfluorobutane. Interestingly, Benton *et al.*, and the results presented herein both show similar oxygen scavenging with the partial pressure decreasing from approximately 550 mmHg to approximately 150 mmHg. In addition, Stone *et al.*[16] showed increased transition efficiency when using PFB. They also found that the calculated transition efficiency at 0.5×10^{-4} mL mL^{-1} was 69% ± 4% higher than 44% ± 9% at 5×10^{-4} mL mL^{-1}. Analogous observations regarding transition efficiency for different perfluorocarbons were made by Moncion *et al.* for perfluoropentane and perfluorohexane double emulsions.

Oxygen scavenging observed *in vitro* was greater than that observed *ex vivo* for the same emulsion concentrations. Specifically, at shared concentrations of 0.25×10^{-4}, 0.5×10^{-4}, and 2.5×10^{-4} mL mL^{-1}, the magnitude of oxygen scavenging *in vitro* was approximately 150 ± 41, 208 ± 9, and 329 ± 37 mmHg, respectively, compared to *ex vivo* values of 85 ± 17, 94 ± 14, and 185 ± 31 mmHg, respectively. This result may be due to a limitation in the oxygen flow sensors, which have a response time on the order of tens of seconds. Fig. 9 demonstrates that the oxygen partial pressure did not achieve sustained steady-state values, which were observed in the *in vitro* experiments where ultrasound insonation lasted for a longer period, with 2 full minutes for *in vitro* and 1 minute for *ex vivo*, taking into consideration the 1-minute delay. The time to achieve a steady state value will be influenced by the response time of the oxygen sensors. Furthermore, the mixing of fluids may also impact the readout because the buffer does not follow plug-flow conditions. Additionally, the macrobubble trap and its opening to atmospheric conditions to achieve constant perfusion pressure resulted in the buffer being briefly exposed to air, which may result in gas exchange. The *in vitro* experiments allowed us to isolate and compare the impacts of spontaneous (*i.e.*, without ultrasound) droplet vaporization and acoustic droplet vaporization. Spontaneous vaporization refers to the spontaneous transition of PFC from a liquid state to a gaseous state without the application of ultrasound.[75] Separating the effects of spontaneous *versus* acoustic droplet vaporization was not feasible in the *ex vivo* setup because of the potential hysteretic response of the heart. The *in vitro* experimental setup also enabled measurement of transition efficiency, allowing comparison with results from Stone *et al.*[16] and Benton *et al.*[15] for various perfluorocarbon droplet sizes.

Notably, findings described in this study suggest that ADV-based controlled hypoxic reperfusion may be a feasible approach to cardioprotection, as the magnitude of oxygen scavenging observed at 2.5×10^{-4} mL mL^{-1} *in vitro* is similar to the magnitude of oxygen used by Fischesser *et al.*[7] to demonstrate cardioprotection *via* controlled hypoxic reperfusion.[7] This discussion would be relevant in future studies exploring whether the observed oxygen scavenging is sufficient to predict cardioprotection based on findings from Fischesser *et al.*[7] Additionally, Stone *et al.*[16] found that a droplet concentration of 0.50×10^{-4} mL mL^{-1} provided sufficient oxygen scavenging, correlating with the cardioprotection observed by Fischesser *et al.*[7] These findings indicate that the current study's results, which

suggest that lower droplet concentrations are adequate, are promising. However, a comprehensive safety evaluation must also be considered to assess the potential toxicological effects of PFC droplets on vital organs, particularly the lungs and liver. This involves *in vitro* studies to measure cytotoxicity and inflammatory responses in lung and liver[76] cell lines, as well as *in vivo* studies using animal models to track biodistribution, clearance, and accumulation.[77] Histopathological examinations and biochemical assays may be needed to identify any morphological changes or functional impairments in these organs.[78] Advanced imaging techniques like MRI and ultrasound can be utilized to monitor the behavior of PFC droplets in real time.[79] These evaluations ensure that any necessary modifications to the droplet formulation or dosing regimen can be made to guarantee safety.[80] A dosing safety evaluation must also be considered by taking into account that our PFC droplet concentration (5×10^{-5} mL mL^{-1}) is higher than that of commonly used ultrasound contrast agents,[81] such as Definity® (8.34×10^{-6} mL mL^{-1}), Optison™ (0.62 to 2.35×10^{-7} mL mL^{-1}), and Lumason® (2.62 to 4.19×10^{-7} mL mL^{-1}). However, it was two orders of magnitude lower than the clinical PFC concentration used for the blood substitute Fluosol-DA (20%), 2.6×10^{-2} mL of PFC per mL of L of PFC per mL of blood.[22–24,82,83] A more thorough assessment of PFC dose, specific to the type of PFC used, will be crucial for assessing safety and refining clinical potential.

The decrease in P_{O_2} due to droplets without ultrasound exposure was expected due to the solubility of oxygen in liquid perfluorobutane and possible spontaneous vaporization.[14] This observation was reported by Stone *et al.*[16] For all concentrations above 0.05×10^{-4} mL mL^{-1}, the oxygen scavenging due to ADV was significantly greater than from spontaneous droplet vaporization. These results indicate that spontaneous droplet vaporization's role in oxygen scavenging is minimal except at the lowest concentration. Recommendations for future cardioprotection studies should aim to optimize droplet concentration and size to achieve sufficient oxygen scavenging for therapeutic efficacy while prioritizing safety, with a balanced approach that considers the differences observed between *in vitro* and *ex vivo* experiments. For the PFB droplet formulation used here, a possible cardioprotection study might be performed using a target concentration of 1.5×10^{-4} mL mL^{-1}.

Transition efficiency

The transition efficiency, defined as the number fraction of droplets that vaporize,[47] was calculated based on the magnitude of oxygen scavenged and initial droplet concentration using the model of Radhakrishnan *et al.*[14] The transition efficiency was found to increase with increasing droplet concentration between 0.05×10^{-4}, 0.25×10^{-4}, and 0.5×10^{-4} mL mL^{-1}, and to decrease as the concentration was further increased to 2.5×10^{-4}, 5×10^{-4} mL mL^{-1} (Fig. 10). The finding that transition efficiency depends on concentration is consistent with the results of Benton *et al.* for PFP droplets[14] and Stone *et al.*[16] for PFB droplets.

Stone *et al.*,[16] using the same PFB droplet manufacturing protocol and ultrasound insonation as this study, measured transition efficiency as a function of droplet diameter. Their observation that larger droplets vaporize more readily was consistent with Fabiilli *et al.*[47] and Benton *et al.*[15] Analysis of the results of Stone *et al.*[16] shows that 55 ± 5% of the PFB volume phase transitioned corresponded to droplets smaller than 1 μm at concentrations of 0.5×10^{-4} mL mL^{-1}. Because the magnitude of oxygen scavenging scales with the volume of perfluorocarbon phase transitioned[14] these results demonstrate that droplets smaller than 1 μm contribute to oxygen scavenging of 37 ± 13%.

Limitations

A limitation of this study is that the Multisizer could not measure the complete size distribution of PFB droplets. The smallest measurable diameter was 0.40 μm (based on the using a 20 μm aperture). Based on flow cytometry measurements by Stone *et al.*[16] 0.3–0.4% of droplets were smaller than 0.40 μm. This limitation affects not only the accuracy of the size distribution but also the determination of the concentration, polydispersity index, and transition efficiency. As a result, the characterization of the droplets may not be fully representative of their actual distribution.

The use of the Langendorff model in this study allowed for the assessment of oxygen scavenging magnitude and the risk of gas embolization. However, there are several limitations associated with the Langendorff model. Due to cumulative effects on a heart during an experiment, it was impossible to separately measure the effect of droplets alone from droplets exposed to ultrasound within the same trial. This model, while replicating many biological aspects of coronary flow and cardiac function, inherently lacks the complexity of a full *in vivo* physiological context. The model does not replicate how the droplets would interact with the heart in the presence of circulating blood. These effects include the non-Newtonian fluid properties of blood and the oxygen carrying capacity of whole blood.[84]

Moreover, the study investigated one species but it is known that there are differences in microvasculature diameter across various species.[85,86] Henquell *et al.*[86] reported the mean diameter in rat heart capillaries to be 4.41 ± 0.09 μm, Hogg *et al.*[87] reported the mean diameters of the pulmonary capillaries to be 7.1 ± 2.6 μm, whereas Tillmanns *et al.*[85] reported the mean diameter in capillaries to be 4–6 μm in dogs. Furthermore, variations in the capillary diameter have been observed within the same species between the systolic and diastolic phases of the cardiac cycle. Tillmanns *et al.*[85] documented that the capillary diameter during the systolic phase was 4.1 ± 0.6 μm in dogs, respectively, while during the diastolic phase, it was 6.3 ± 0.6 μm. These differences might affect the droplet concentration and modal diameter where gas embolism occurs, particularly for *in vivo* models, which in turn would impact the selection of experimental parameters for future cardioprotection studies.

Another limitation of this study was the dependence on bubbling for controlling the oxygenation of the KHB. The fluctuations in oxygenation could have affected the

consistency of the experimental conditions, potentially influencing the results.

A final limitation of this study is that it focused on cardiac function and perfusion. Other tissue changes, such as those induced by transient ischemia from gas embolism, may have occurred. Future research using histological or other assays would complement the functional observations of this study.

Conclusions

In this study, we have demonstrated that it is possible to scavenge oxygen using low boiling point PFB droplets in *ex vivo* and *in vitro* models. The results show that droplet concentration impacts both the magnitude of oxygen scavenging and also the risk of gas embolization in an *ex vivo* rat heart. The presented results indicate that the magnitude of oxygen scavenging increased when the infused perfluorobutane droplet concentration increased from 0.05×10^{-4} mL mL^{-1} to 5×10^{-4} mL mL^{-1}. These results indicate the oxygen scavenging effect can be modulated by varying the droplet concentration. The heart function showed recovery paired with oxygen scavenging ability when using 0.25×10^{-4} mL mL^{-1}, 0.5×10^{-4} mL mL^{-1}, and 1.5×10^{-4} mL mL^{-1} and occluded when using 2.5×10^{-4} mL mL^{-1} and 5×10^{-4} mL mL^{-1}. The oxygen scavenging increased as we increased the droplet concentration, where it was 85 mmHg for 0.25×10^{-4} mL mL^{-1}, 94 mmHg for 0.5×10^{-4} mL mL^{-1}, and 143 mmHg for 1.5×10^{-4} mL mL^{-1}. In addition, the droplet transition efficiency exhibited a peak value at a droplet concentration of 0.5×10^{-4} mL mL^{-1}.

Author contributions

N. A. R., K. J. H., and A. N. R. contributed to the study of conceptualization and experimental design. N. A. R., B. B. and K. S. performed experiments. N. A. R., D. K., and K. J. H. wrote software for data processing. N. A. R., B. Z., and K. J. H. performed the formal analysis. N. A. R. and K. J. H. prepared the original draft. All authors assisted with editing and reviewing. K. J. H. was responsible for funding acquisition and project administration.

Data availability

The data supporting this article have been published on Scholar@UC and are available at: **https://scholar.uc.edu/collections/1g05fd126**.

Conflicts of interest

K. J. H. previously served as a consultant for Boston Scientific Inc. Other co-authors have no relevant conflicts to declare.

Acknowledgements

This work was supported by the National Heart, Lung, and Blood Institute of the National Institutes of Health under award number R01HL148451. The authors acknowledge Professor Christy Holland at the University of Cincinnati for assistance with Multisizer sizing.

References

1 G. Heusch, *Nat. Rev. Cardiol.*, 2020, **17**, 773–789.
2 D. M. Yellon and D. J. Hausenloy, *N. Engl. J. Med.*, 2007, **357**, 1121–1135.
3 D. J. Hearse, S. M. Humphrey and E. B. Chain, *J. Mol. Cell. Cardiol.*, 1973, **5**, 395–407.
4 M. L. Hess and N. H. Manson, *J. Mol. Cell. Cardiol.*, 1984, 969–985.
5 D. N. Granger and P. R. Kvietys, *Redox Biol.*, 2015, **6**, 524–551.
6 H. Fu, J. Fu, S. Ma, H. Wang, S. Lv and Y. Hao, *J. Mater. Chem. B*, 2020, **8**, 6059–6068.
7 D. M. Fischesser, B. Bo, R. P. Benton, H. Su, N. Jahanpanah and K. J. Haworth, *J. Cardiovasc. Pharmacol. Ther.*, 2021, **26**, 504–523.
8 E. Farine, P. Niederberger, R. K. Wyss, N. Méndez-Carmona, B. Gahl, G. M. Fiedler, T. P. Carrel, H. T. Tevaearai Stahel and S. L. Longnus, *Frontiers*, 2016, **7**, 26–36.
9 R. E. Apfel, Activatable infusable dispersions containing drops of a superheated liquid for methods of therapy and diagnosis, US5840276A, **https://patents.google.com/patent/US5840276A/en**, (accessed January 2, 2020).
10 N. Y. Rapoport, A. M. Kennedy, J. E. Shea, C. L. Scaife and K.-H. Nam, *J. Controlled Release*, 2009, **138**, 268–276.
11 K. Kawabata, N. Sugita, H. Yoshikawa, T. Azuma and S. Umemura, *Jpn. J. Appl. Phys.*, 2005, **44**, 4548.
12 O. D. Kripfgans, J. B. Fowlkes, D. L. Miller, O. P. Eldevik and P. L. Carson, *Ultrasound Med. Biol.*, 2000, **26**, 1177–1189.
13 T. Giesecke and K. Hynynen, *Ultrasound Med. Biol.*, 2003, **29**, 1359–1365.
14 K. Radhakrishnan, C. K. Holland and K. J. Haworth, *Ultrason. Sonochem.*, 2016, **31**, 394–403.
15 R. P. Benton, N. Al Rifai, K. Stone, A. Clark, B. Zhang and K. J. Haworth, *Pharmaceutics*, 2022, **14**, 2392.
16 K. Stone, N. Al Rifai, D. M. Fischesser, J. Dumancic, S. Abid, D. Willett, C. K. Holland and K. J. Haworth, *Ultrasound Med. Biol.*, 2025, **51**, 402–413.
17 K. J. Haworth, C. K. Holland, K. P. Mercado-Shekhar, A. N. Redington and B. H. Goldstein, Intravascular ultrasound device and methods for avoiding or treating reperfusion injury, US11950792B2, 2024.
18 S.-T. Kang, Y.-L. Huang and C.-K. Yeh, *Ultrasound Med. Biol.*, 2014, **40**, 551–561.
19 P. S. Sheeran, V. P. Wong, S. Luois, R. J. McFarland, W. D. Ross, S. Feingold, T. O. Matsunaga and P. A. Dayton, *Ultrasound Med. Biol.*, 2011, **37**, 1518–1530.
20 J. L. H. Johnson, M. C. Dolezal, A. Kerschen, T. O. Matsunaga and E. C. Unger, *Artif. Cells, Blood Substitutes, Biotechnol.*, 2009, **37**, 156–162.
21 W. C. Culp, S. D. Woods, R. D. Skinner, A. T. Brown, J. D. Lowery, J. L. H. Johnson, E. C. Unger, L. J. Hennings,

M. J. Borrelli and P. K. Roberson, *J. Vasc. Interventional Radiol.*, 2012, **23**, 116–121.
22 M. P. Krafft and J. G. Riess, *Adv. Colloid Interface Sci.*, 2021, **294**, 102407.
23 R. Lustig, N. McIntosh-Lowe, C. Rose, J. Haas, S. Krasnow, M. Spaulding and L. Prosnitz, *Int. J. Radiat. Oncol., Biol., Phys.*, 1989, **16**, 1587–1593.
24 T. Mitsuno, H. Ohyanagi and R. Naito, *Ann. Surg.*, 1982, **195**, 60–69.
25 K. P. Mercado-Shekhar, H. Su, D. S. Kalaikadal, J. N. Lorenz, R. M. Manglik, C. K. Holland, A. N. Redington and K. J. Haworth, *Ultrason. Sonochem.*, 2019, **56**, 114–124.
26 N. Reznik, R. Williams and P. N. Burns, *Ultrasound Med. Biol.*, 2011, **37**, 1271–1279.
27 P. S. Sheeran, V. P. Wong, S. Luois, R. J. McFarland, W. D. Ross, S. Feingold, T. O. Matsunaga and P. A. Dayton, *Ultrasound Med. Biol.*, 2011, **37**, 1518–1530.
28 P. S. Sheeran, J. E. Streeter, L. B. Mullin, T. O. Matsunaga and P. A. Dayton, *Ultrasound Med. Biol.*, 2013, **39**, 893–902.
29 P. S. Sheeran, J. D. Rojas, C. Puett, J. Hjelmquist, C. B. Arena and P. A. Dayton, *Ultrasound Med. Biol.*, 2015, **41**, 814–831.
30 P. S. Sheeran, Y. Daghighi, K. Yoo, R. Williams, E. Cherin, F. S. Foster and P. N. Burns, *Ultrasound Med. Biol.*, 2016, **42**, 795–807.
31 P. S. Sheeran, N. Matsuura, M. A. Borden, R. Williams, T. O. Matsunaga, P. N. Burns and P. A. Dayton, *IEEE Trans. Ultrason. Ferroelectr. Freq. Control*, 2017, **64**, 252–263.
32 J. A. Kopechek, E.-J. Park, Y.-Z. Zhang, N. I. Vykhodtseva, N. J. McDannold and T. M. Porter, *Phys. Med. Biol.*, 2014, **59**, 3465.
33 L. C. Moyer, K. F. Timbie, P. S. Sheeran, R. J. Price, G. W. Miller and P. A. Dayton, *J. Ther. Ultrasound*, 2015, **3**, 7.
34 D. Pajek, A. Burgess, Y. Huang and K. Hynynen, *Ultrasound Med. Biol.*, 2014, **40**, 2151–2161.
35 M. Zhang, M. L. Fabiilli, K. J. Haworth, F. Padilla, S. D. Swanson, O. D. Kripfgans, P. L. Carson and J. B. Fowlkes, *Acad. Radiol.*, 2011, **18**, 1123–1132.
36 P. Zhang and T. Porter, in *2009 IEEE 35th Annual Northeast Bioengineering Conference*, 2009, pp. 1–2.
37 K. J. Haworth, J. B. Fowlkes, P. L. Carson and O. D. Kripfgans, *Ultrasound Med. Biol.*, 2008, **34**, 435–445.
38 M. Zhang, M. L. Fabiilli, K. J. Haworth, J. B. Fowlkes, O. D. Kripfgans, W. W. Roberts, K. A. Ives and P. L. Carson, *Ultrasound Med. Biol.*, 2010, **36**, 1691–1703.
39 O. D. Kripfgans, C. M. Orifici, P. L. Carson, K. A. Ives, O. P. Eldevik and J. B. Fowlkes, *IEEE Trans. Ultrason. Eng.*, 2005, **52**, 1101–1110.
40 R. Díaz-López, N. Tsapis and E. Fattal, *Pharm. Res.*, 2010, **27**, 1–16.
41 C.-Y. Lin and W. G. Pitt, *BioMed Res. Int.*, 2013, **2013**, e404361.
42 M. L. Fabiilli, M. R. Piert, R. A. Koeppe, P. S. Sherman, C. A. Quesada and O. D. Kripfgans, *Contrast Media Mol. Imaging*, 2013, **8**, 366–374.
43 S. Samuel, A. Duprey, M. L. Fabiilli, J. L. Bull and J. B. Fowlkes, *Microcirculation*, 2012, **19**, 501–509.
44 J. S. Harmon, F. Kabinejadian, R. Seda, M. L. Fabiilli, S. Kuruvilla, C. C. Kuo, J. M. Greve, J. B. Fowlkes and J. L. Bull, *Sci. Rep.*, 2019, **9**, 11040.
45 O. D. Kripfgans, J. B. Fowlkes, M. Woydt, O. P. Eldevik and P. L. Carson, *IEEE Trans. Ultrason. Eng.*, 2002, **49**, 726–738.
46 R. Seda, D. S. Li, J. B. Fowlkes and J. L. Bull, *Ultrasound Med. Biol.*, 2015, **41**, 3241–3252.
47 M. L. Fabiilli, K. J. Haworth, I. E. Sebastian, O. D. Kripfgans, P. L. Carson and J. B. Fowlkes, *Ultrasound Med. Biol.*, 2010, **36**, 1364–1375.
48 M. E. Reichelt, L. Willems, B. A. Hack, J. N. Peart and J. P. Headrick, *Exp. Physiol.*, 2009, **94**, 54–70.
49 M. Lafond, N. G. Salido, K. J. Haworth, A. S. Hannah, G. P. Macke, C. Genstler and C. K. Holland, *Ultrasound Med. Biol.*, 2021, **47**, 693–709.
50 S. R. Kennedy, M. Lafond, K. J. Haworth, D. S. Escudero, D. Ionascu, B. Frierson, S. Huang, M. E. Klegerman, T. Peng, D. D. McPherson, C. Genstler and C. K. Holland, *Sci. Rep.*, 2023, **13**, 6191.
51 D. Suarez Escudero, K. J. Haworth, C. Genstler and C. K. Holland, *Ultrasound Med. Biol.*, 2023, **49**, 2388–2397.
52 R. M. Bell, M. M. Mocanu and D. M. Yellon, *J. Mol. Cell. Cardiol.*, 2011, **50**, 940–950.
53 J. C. Fasciolo and H. Chiodi, *Am. J. Physiol.*, 1946, **147**, 54–65.
54 C. Christoforides, L. H. Laasberg and J. Hedley-Whyte, *J. Appl. Physiol.*, 1969, **26**, 56–60.
55 National Industrial Chemicals Notification and Assessment Scheme, Full Public Report: Perfluorobutane, Government of Australia, Jul. 1996.
56 Perfluorobutane (Decafluorobutane) CAS Number, **https://fluoromed.com/products/perfluorobutane-decafluorobutane-cas-number-355-25-9**, (accessed February 12, 2024).
57 E. Hvattum, P. Trygve Normann, I. Oulie, S. Uran, O. Ringstad and T. Skotland, *J. Pharm. Biomed. Anal.*, 2001, **24**, 487–494.
58 K. A. Reimer and R. B. Jennings, *Lab. Invest.*, 1979, **40**, 633–644.
59 N. Matsuura, R. Williams, I. Gorelikov, J. Chaudhuri, J. Rowlands, K. Hynynen, S. Foster, P. Burns, N. Resnik, J. Rowlands, K. Hynynen, S. Foster and P. Burns, in *2009 IEEE International Ultrasonics Symposium*, 2009, pp. 5–8.
60 C. M. Muth and E. S. Shank, *N. Engl. J. Med.*, 2000, **342**, 476–482.
61 C. de Gracia Lux, A. M. Vezeridis, J. Lux, A. M. Armstrong, S. R. Sirsi, K. Hoyt and R. F. Mattrey, *RSC Adv.*, 2017, **7**, 48561–48568.
62 M. P. Nikolova, E. M. Kumar and M. S. Chavali, *Pharmaceutics*, 2022, **14**, 2195.
63 P. S. Sheeran, S. H. Luois, L. B. Mullin, T. O. Matsunaga and P. A. Dayton, *Biomaterials*, 2012, **33**, 3262–3269.
64 S. F. Sadeghian, M. Majdinasab, M. Nejadmansouri and S. M. H. Hosseini, *Ultrason. Sonochem.*, 2022, **92**, 106277.
65 D. S. Li, S. Schneewind, M. Bruce, Z. Khaing, M. O'Donnell and L. Pozzo, *Nano Lett.*, 2019, **19**, 173–181.
66 M. Aliabouzar, O. D. Kripfgans, W. Y. Wang, B. M. Baker, J. Brian Fowlkes and M. L. Fabiilli, *Ultrason. Sonochem.*, 2021, **72**, 105430.

67 A. Woodward, R. F. Mattrey and C. de Gracia Lux, *Ultrasound Med. Biol.*, 2024, **50**, 445–452.
68 S. G. Ting, H. Lea-Banks and K. Hynynen, *Pharmaceutics*, 2023, **15**, 2077.
69 S. K. Yarmoska, H. Yoon and S. Y. Emelianov, *Ultrasound Med. Biol.*, 2019, **45**, 1489–1499.
70 H. E. Bøtker, D. Hausenloy, I. Andreadou, S. Antonucci, K. Boengler, S. M. Davidson, S. Deshwal, Y. Devaux, F. Di Lisa, M. Di Sante, P. Efentakis, S. Femminò, D. García-Dorado, Z. Giricz, B. Ibanez, E. Iliodromitis, N. Kaludercic, P. Kleinbongard, M. Neuhäuser, M. Ovize, P. Pagliaro, M. Rahbek-Schmidt, M. Ruiz-Meana, K.-D. Schlüter, R. Schulz, A. Skyschally, C. Wilder, D. M. Yellon, P. Ferdinandy and G. Heusch, *Basic Res. Cardiol.*, 2018, **113**, 39.
71 S. Sasayama, H. Nonogi, S. Miyazaki, T. Sakurai, C. Kawai, S. Eiho and M. Kuwahara, *J. Am. Coll. Cardiol.*, 1985, **5**, 599–606.
72 T. Serizawa, W. M. Vogel, C. S. Apstein and W. Grossman, *J. Clin. Invest.*, 1981, **68**, 91–102.
73 S. Sabnis, E. S. Kumarasinghe, T. Salerno, C. Mihai, T. Ketova, J. J. Senn, A. Lynn, A. Bulychev, I. McFadyen, J. Chan, Ö. Almarsson, M. G. Stanton and K. E. Benenato, *Mol. Ther.*, 2018, **26**, 1509–1519.
74 Y. Y. C. Tam, S. Chen and P. R. Cullis, *Pharmaceutics*, 2013, **5**, 498–507.
75 P. S. Sheeran, S. H. Luois, L. B. Mullin, T. O. Matsunaga and P. A. Dayton, *Biomaterials*, 2012, **33**, 3262–3269.
76 Y. Xiang, N. Bernards, B. Hoang, J. Zheng and N. Matsuura, *Nanotheranostics*, 2019, **3**, 135–144.
77 Safety evaluation of superheated perfluorocarbon nanodroplets for novel phase change type neurological therapeutic agents – ScienceDirect, **https://www-sciencedirect-com.uc.idm.oclc.org/science/article/pii/S2211968X12000654?utm_source=chatgpt.com**, (accessed March 19, 2025).
78 J. Shimizu, R. Endoh, T. Fukuda, T. Inagaki, H. Hano, R. Asami, K. Kawabata, M. Yokoyama and H. Furuhata, *Perspect. Med.*, 2012, **1**, 25–29.
79 P. A. Dayton, S. Zhao, S. H. Bloch, P. Schumann, K. Penrose, T. O. Matsunaga, R. Zutshi, A. Doinikov and K. W. Ferrara, *Mol. Imaging*, 2006, **5**, 160–174.
80 N. Kakaei, R. Amirian, M. Azadi, G. Mohammadi and Z. Izadi, *Front. Bioeng. Biotechnol.*, 2023, **11**, DOI: **10.3389/fbioe.2023.1115254**.
81 A. Sridharan, J. R. Eisenbrey, F. Forsberg, N. Lorenz, L. Steffgen and A. Ntoulia, *Pediatr. Radiol.*, 2021, **51**, 2117–2127.
82 S. A. Gould, A. L. Rosen, L. R. Sehgal, H. L. Sehgal, L. A. Langdale, L. M. Krause, C. L. Rice, W. H. Chamberlin and G. S. Moss, *N. Engl. J. Med.*, 1986, **314**, 1653–1656.
83 L. Oberholzer, D. Montero, P. Robach, C. Siebenmann, C. K. Ryrsøe, T. C. Bonne, A. Breenfeldt Andersen, J. Bejder, T. Karlsen, E. Edvardsen, B. R. Rønnestad, H. Hamarsland, A. C. Cepeda-Lopez, J. Rittweger, G. Treff, C. Ahlgrim, N. W. Almquist, J. Hallén and C. Lundby, *Am. J. Hematol.*, 2024, **99**, 88–98.
84 K. Stone, N. Al Rifai, D. M. Fischesser, J. Dumancic, S. Abid, D. Willett, C. K. Holland and K. J. Haworth, *Ultrasound Med. Biol.*, 2025, **51**(2), 402–413.
85 H. Tillmanns, S. Ikeda, H. Hansen, J. S. Sarma, J. M. Fauvel and R. J. Bing, *Circ. Res.*, 1974, **34**, 561–569.
86 L. Henquell, P. L. LaCelle and C. R. Honig, *Microvasc. Res.*, 1976, **12**, 259–274.
87 C. M. Doerschuk, N. Beyers, H. O. Coxson, B. Wiggs and J. C. Hogg, *J. Appl. Physiol.*, 1993, **74**, 3040–3045.

